University College London

MATHM901: **Final Year Project**

Application of Similarity Solutions in the Frictional Dam-Break Problem

Mr. William Jackman
Supervisor:
Prof. Gavin Esler

March 9, 2017

Contents

1 Introduction **3**

2 Modelling Friction in the Shallow Water Equations **4**
2.1 Governing equations and non-dimensionalisation 4
2.2 Solving at first order for a small friction coefficient 6
2.3 Similarity solutions 7

3 Wet Dam-Break Problem **8**
3.1 Set up and initial conditions 8
3.2 Linearisation at far ends of the domain 9
3.3 Numerical solutions of (12) for the wet dam-break 11

4 Dry Dam-Break Problem **16**
4.1 Set up and initial conditions 16
4.2 Solution near the wave front 16
4.3 Numerical solutions of (12) for the dry dam-break 17

5 Front Velocity at Small Times **22**
5.1 Whitham's solution for Chézy friction 22
5.2 Adjusting Whitham's solution for general friction 25
5.3 Asymptotic behaviour of (65)'s solutions 31
5.4 Comparison of Manning and Chézy friction 34
5.5 Asymptotic behaviour at the back of the tip region 34

6 Rescaling **36**

7 Concluding Remarks **37**

8 Appendix **38**

A Appendix A **38**
A.1 Frictionless Shallow Water Equations 38
A.2 Secant method 38
A.3 Ritter solution for the frictionless shallow water equations . 38

B MATLAB codes **39**
B.1 MATLAB code to solve (12) 39
B.2 MATLAB code to solve (65) 42

References **44**

Acknowledgments

I would like to express my gratitude to Prof. Gavin Esler for his insight and enthusiasm during the development of this project. His generosity of time and relentless passion for the subject area has been very much appreciated.

My grateful thanks are also extended to the resources and opportunities made available by University College London.

Special thanks are given to my family for their continual support and encouragement in all that I do.

1 Introduction

If the wall of a dam instantaneously breaks, how fast will the flood spread? How deep will the flooding be? Understanding the dynamics of a dam failure is critical for risk-assessment of areas near dams.

Typically, to answer these questions, shallow water theory is introduced and the dam-break problem is solved numerically. However, near to the front of the flow, numerical instabilities commonly arise. Hence, analytical results are important to test the robustness of computational models.

Assuming an infinite stretch of fluid behind a dam on a flat frictionless base, Ritter (1892) [1] analytically solved an idealised version of the dam-break problem which is regularly used and referred to. Using perturbation theory, Dressler (1952) [2] found an approximate solution for the velocity of the wave front if Chézy friction is introduced to the system. This prompted a momentous paper by Whitham (1955) [3], where an improved solution for the front speed under Chézy friction was found. Exact analytical solutions for a finite volume dam-break on a sloped frictionless base have been addressed by Ancey et al. (2008) [4]. Analytical solutions for various sloping and flat based frictional dam-breaks are given by Chanson (2009) [5] using the method of characteristics.

This study first investigates the long time asymptotic behaviour of the flat based frictional dam-break problem. Shallow water theory is assumed and friction is modelled by a quadratic friction term divided by some power of the height of the flow (of which a particular case is Chézy friction). Taking inspiration from Daley and Porporato (2004) [6], self-similar solutions are found and in the dry dam-break problem. These ultimately yield a result for the long time propagation speed of the wave front.

In section 5, the study aims to find the small time asymptotics for the same dry dam-break problem using the method adopted by Whitham (1955) [3]. Complications of the method arise when considering the more general friction strength and a reasonable fix for this is addressed. Asymptotic analysis of the solutions obtained in this section ultimately find some interesting results and highlight some of the pitfalls of Whitham's method. It is worth noting, however, a more mathematically rigorous approach to Whitham's method may be found in Hogg and Pritchard (2004) [7].

2 Modelling Friction in the Shallow Water Equations

2.1 Governing equations and non-dimensionalisation

Assuming no Coriolis or viscous forces, we start with the frictional one dimensional shallow water equations for unknowns $u(x,t)$ and $h(x,t)$, the depth-averaged fluid velocity and height of the fluid above the topography $b(x)$ respectively; where $b(x)$ is some specified height for the base of the flow (which we will later take as a constant). In non-conservative form the frictional one dimensional shallow water equations are

$$h_t + (uh)_x = 0, \tag{1}$$

$$u_t + uu_x = -g\left(h_x + b_x + \frac{u|u|}{C^2 h^\alpha}\right). \tag{2}$$

Here, α is some real constant which we will decide later.

The final term in (2) used to model the friction on the fluid from the base of the flow (a review of the *frictionless* shallow water equations can be found in appendix A.1). Two commonly used forms of the friction term are

$$\begin{array}{ll} \alpha = 1 & \text{(Chézy friction), and} \\ \alpha = 4/3 & \text{(Manning friction).} \end{array}$$

If $\alpha = 1$, then $C = C_f$, where C_f is the Chézy friction coefficient. If $\alpha = 4/3$, then $C = 1/n_M$ where n_M is the Gauckler-Manning coefficient [8]. Although we will consider a general α in the theory that follows, there will be particular interest and comparison of the Chézy and Manning cases throughout. Chézy's friction term is formed on the basis that (2) multiplied by h gives the momentum balance for a vertical column; Chézy resistance is found by assuming the resistance force on a vertical column will be proportional to u^2. Dividing through by h gives (2) with $\alpha = 1$. Introducing alternative α values is the same as modelling the resistance on a vertical section of the flow as proportional to u^2, however the proportionality may vary with a power of h (namely, $h^{1-\alpha}$). It has also been shown by Gioia and Bombardelli (2001) [9] that the '4/3' value of α for Manning friction has theoretical grounds for turbulent flow.

We non-dimensionalise the equations by letting L be a typical x length scale and H_1 a typical h length scale. Balancing the uu_x and gh_x terms in (2) implies $\sqrt{(gH_1)}$ is a typical velocity. Time can found as length divided by velocity and thus $L/\sqrt{(gH_1)}$ is taken as a typical time (this is also consistent with balancing the terms in the mass conservation equation

(1)). Letting

$$\begin{aligned} x &= L\bar{x}, \\ h &= H_1\bar{h}, \\ b &= H_1\bar{b}, \\ u &= \sqrt{(gH_1)}\bar{u}, \\ t &= \frac{L}{\sqrt{(gH_1)}}\bar{t}, \end{aligned} \tag{3}$$

for dimensionless variables $\bar{x}$, $\bar{h}$, $\bar{b}$, $\bar{u}$ and $\bar{t}$, the momentum conservation equation (2) transforms to give

$$\bar{u}_{\bar{t}} + \bar{u}\bar{u}_{\bar{x}} = -(\bar{h}_{\bar{x}} + \bar{b}_{\bar{x}}) - \frac{gL}{C^2 H_1^{\alpha}} \frac{\bar{u}|\bar{u}|}{\bar{h}^{\alpha}}. \tag{4}$$

Let's define a variable r by

$$\frac{1}{r^2} = \frac{gL}{C^2 H_1^{\alpha}}. \tag{5}$$

Then, since all terms of (4) must have the same dimensions, we find

$$1 = \left[\frac{gL}{C^2 H_1^{\alpha}}\right] = \left[\frac{1}{r^2}\right],$$

and hence r is a dimensionless variable. We will refer to r as the 'friction coefficient'. The friction coefficient is analogous to the Reynolds number for the Navier-Stokes equations and, like the Reynolds number, the friction coefficient holds the relation between the properties of similar flows. Explicitly,

$$r = \left(\frac{H_1^{\alpha}}{gL}\right)^{\frac{1}{2}} C. \tag{6}$$

Noting that the mass conservation equation remains the same in dimensionless variables, the frictional shallow water equations (1) and (2) may now be written in the fully dimensionless form

$$\begin{aligned} \bar{h}_{\bar{t}} + (\bar{u}\bar{h})_{\bar{x}} &= 0, \\ \bar{u}_{\bar{t}} + \bar{u}\bar{u}_{\bar{x}} &= -(\bar{h}_{\bar{x}} + \bar{b}_{\bar{x}}) - \frac{\bar{u}|\bar{u}|}{r^2 \bar{h}^{\alpha}}. \end{aligned}$$

From here on we drop the bar notation for readability with the understanding that any variables appearing are dimensionless, i.e.

$$h_t + (uh)_x = 0, \tag{7}$$

$$u_t + uu_x = -(h_x + b_x) - \frac{u|u|}{r^2 h^{\alpha}}. \tag{8}$$

2.2 Solving at first order for a small friction coefficient

If we have a free choice of L, relation (6) implies we can scale in the x direction such that r^2 is any positive value desired. In particular, an arbitrarily large L (and consequently an arbitrarily large T) will give rise to an arbitrarily small friction coefficient. Then, as a first step to solving the shallow water equations (7) and (8) we may expand u about r as follows

$$u(x,t) = r\left(u_0(x,t) + ru_1(x,t) + r^2u_2(x,t) + \cdots\right).$$

Substituting the series into (8) and equating at leading order we get

$$0 = -\left(h_x + b_x\right) - \frac{u_0|u_0|}{h^\alpha},$$

which we can solve for u_0 as

$$u_0 = -\mathrm{sgn}(h_x + b_x)|h_x + b_x|^{\frac{1}{2}}h^{\frac{\alpha}{2}}. \tag{9}$$

Substituting (9) into the mass conservation equation (7) gives

$$h_t - r\mathrm{sgn}(h_x + b_x)\left(|(h_x + b_x)|^{\frac{1}{2}}h^{\frac{\alpha}{2}+1}\right)_x = 0.$$

Expanding using the product rule, and denoting $h + b$ with H, we find

$$\begin{aligned} h_t &= \left(r\mathrm{sgn}(H_x)|H_x|^{\frac{1}{2}}h^{\frac{\alpha}{2}+1}\right)_x \\ &= r\mathrm{sgn}(H_x)\left\{\frac{\mathrm{sgn}(H_x)}{2|H_x|^{\frac{1}{2}}}H_{xx}h^{\frac{\alpha}{2}+1} + (\frac{\alpha}{2}+1)|H_x|^{\frac{1}{2}}h^{\frac{\alpha}{2}}h_x\right\} \\ &= \frac{r}{2|H(x)|^{\frac{1}{2}}}\left\{h^{\frac{\alpha}{2}+1}H_{xx} + (\alpha+2)h^{\frac{\alpha}{2}}h_xH_x\right\}. \end{aligned}$$

We now introduce a flat base by imposing the condition

$$b_x \equiv 0.$$

Thus $H_x = h_x + b_x = h_x$ and we are left with a partial differential equation in $h(x,t)$ and the parameter α only

$$h_t = \frac{rh^{\frac{\alpha}{2}+1}h_{xx}}{2|h_x|^{\frac{1}{2}}} + (\alpha+2)\frac{rh^{\frac{\alpha}{2}}(h_x)^2}{2|h_x|^{\frac{1}{2}}}. \tag{10}$$

This is simply an expanded version of the non-linear diffusion equation

$$h_t = \left(r\mathrm{sgn}(h_x)|h_x|^{\frac{1}{2}}h^{\frac{\alpha}{2}+1}\right)_x.$$

Since this is the leading order equation about $r \ll 1$, solutions to this equation give the solution as $t \to \infty$ by the scaling argument above.

2.3 Similarity solutions

At this point we try seeking a similarity solution as proposed by Daly and Porporato (2004) [6] - that is, we form the ansatz $h(x,t) = F(s)$ where $s = xt^{\beta}$. Letting a dash denote differentiation by s, by the chain rule we have

$$\begin{aligned} h_x &= t^{\beta} F', \\ h_{xx} &= t^{2\beta} F'', \\ h_t &= \beta x t^{\beta-1} F'. \end{aligned}$$

Replacing $h(x,t)$ and all its derivatives in favour of $F(s)$ we find (10) becomes

$$2\frac{\beta x}{r} t^{\frac{3}{2}\beta-1} F'|F'|^{\frac{1}{2}} = t^{2\beta} F^{\frac{\alpha}{2}+1} F'' + t^{2\beta} F^{\frac{\alpha}{2}} (\alpha+2) (F')^2.$$

Eliminating explicit x dependence in favour of s gives

$$2\frac{\beta s}{r} t^{\frac{1}{2}\beta-1} F'|F'|^{\frac{1}{2}} = t^{2\beta} \left\{ F^{\frac{\alpha}{2}+1} F'' + F^{\frac{\alpha}{2}} (\alpha+2) (F')^2 \right\}.$$

To reduce equation (10) into an ordinary differential equation for $F(s)$ we eliminate the explicit dependence on t arising in the coefficients. This is achieved by setting

$$\frac{\beta}{2} - 1 = 2\beta,$$

and it follows

$$\beta = -\frac{2}{3}.$$

Substituting in for β and rearranging, we obtain the following second order, non-linear, ordinary differential equation in $s = xt^{-2/3}$ as

$$F'' = -\frac{4s}{3r} \frac{F'|F'|^{\frac{1}{2}}}{F^{\frac{\alpha}{2}+1}} - (\alpha+2) \frac{(F')^2}{F}. \tag{11}$$

In particular,

$$\begin{aligned} F'' &= -\frac{4s}{3r} \frac{F'|F'|^{\frac{1}{2}}}{F^{3/2}} - 3\frac{(F')^2}{F} \qquad \text{(for Chézy friction, } \alpha = 1), \\ F'' &= -\frac{4s}{3r} \frac{F'|F'|^{\frac{1}{2}}}{F^{5/3}} - \frac{10}{3}\frac{(F')^2}{F} \quad \text{(for Manning friction, } \alpha = 4/3). \end{aligned}$$

Unfortunately, (11) does not have any known non-trivial analytical solutions. However, with the aid of the correct boundary conditions we can solve it numerically.

3 Wet Dam-Break Problem

3.1 Set up and initial conditions

Throughout this section we consider a dam positioned at $x = 0$ holding fluid on both sides which breaks at $t = 0$. We assume the fluid is higher behind the dam ($x < 0$) than in front of the dam ($x > 0$). Suppose, in dimensional variables, the height on the left is H_1 (the typical h length scale introduced earlier) and the height on the right is H_2, where $0 < H_2 < H_1$. In the non-dimensional variables introduced earlier, this gives 1 on the left and h_2 on the right, where $h_2 = H_2/H_1$ (and consequently $0 < h_2 < 1$).

This can be modelled as an initial value problem for $h(x,t)$ by equation (10) together with the initial conditions

$$\begin{cases} h(x,0) = 1 & \text{for} \quad x < 0 \\ h(x,0) = h_2 & \text{for} \quad x > 0, \quad 0 < h_2 < 1. \end{cases}$$

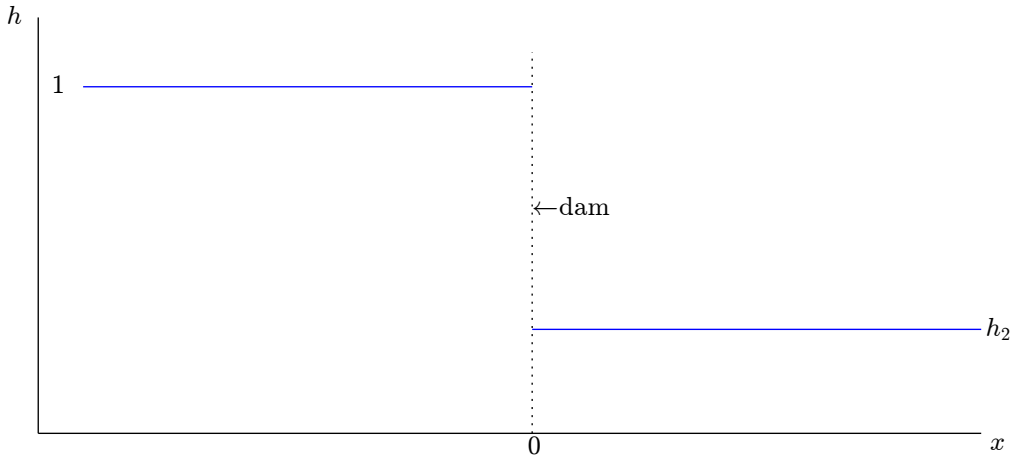

Figure 1: Initial conditions for the wet dam-break.

As shown, this can be converted to equation (11) with the introduction of the function $F(s) = h(x,t)$ with $s = xt^{-\frac{2}{3}}$. The initial conditions on $h(x,t)$ can also be written as boundary conditions on $F(s)$ which converts the dam break problem for $h(x,t)$ entirely into a boundary value problem for $F(s)$. Additionally, since we still have a free choice over the x scaling L, we may assume $r = 1$. Altogether we have

$$F'' = -\frac{4s}{3}\frac{F'|F'|^{\frac{1}{2}}}{F^{\frac{\alpha}{2}+1}} - (\alpha+2)\frac{(F')^2}{F}, \tag{12}$$

$$\begin{cases} F(s) \to 1 & \text{as} \quad s \to -\infty \\ F(s) \to h_2 & \text{as} \quad s \to \infty \end{cases} \quad \text{(boundary conditions on F(s))}. \tag{13}$$

We denote the scaling such that $r = 1$ by a subscript f, to refer to the fact it is a natural '*frictional scale*' for each scaling. Explicitly, (3) and (6) reveal the frictional length and time scales

$$L_f = \frac{C^2 H_1^\alpha}{g}, \tag{14}$$

$$T_f = \frac{C^2 H_1^{\alpha-\frac{1}{2}}}{g^{3/2}}. \tag{15}$$

3.2 Linearisation at far ends of the domain

To solve (12) numerically we need boundary conditions on $F(s)$ at *finite* s values. This is achieved by using (13) together with the intuition that $F'(s)$ must be *small* for large s. We may then solve (12) in regions of large $|s|$ analytically by discarding the negligible terms of the equation. To represent this mathematically, we write

$$F_i^{\text{lin}}(s) = h_i + f_i(s),$$

where $i = 1, 2$, with $i = 1$ and $i = 2$ representing the linearised solution on the left and right respectively. Here, h_1 denotes 1, and f_i is some function of s, presumed to be a *small* height correction at large $|s|$, i.e. $f_i(s) \ll h_i(s)$ for large negative s if $i = 1$ or large positive s if $i = 2$. We calculate

$$\left(F_i^{\text{lin}}(s)\right)' = f_i'(s),$$
$$\left(F_i^{\text{lin}}(s)\right)'' = f_i''(s),$$

and substitution into (12) finds

$$f_i''(s) = -\frac{4s}{3}\frac{f_i'(s)|f_i'(s)|^{\frac{1}{2}}}{h_i^{1+(\alpha/2)}} - (\alpha+2)\frac{(f_i'(s))^2}{h_i}. \tag{16}$$

Here, we have used a result from Taylor series and only kept the h_i term of F_i^{lin} in the denominator since we are interested in the dominant behaviour of each term. The second term on the right hand side of (16) has a higher power of f_i' than the first term on the right hand side. Thus we deem the final term negligible. Balancing the two dominant terms gives

$$f_i''(s) = -\frac{4s}{3}\frac{f_i'(s)|f_i'(s)|^{\frac{1}{2}}}{h_i^{1+(\alpha/2)}}.$$

Integrating over s this becomes

$$\int \frac{f_i''(s)}{|f_i'(s)|^{3/2}} ds = \int \frac{4s}{3h_i^{1+(\alpha/2)}} ds,$$
$$\int \frac{df_i'}{|f_i'|^{3/2}} = \frac{4}{3h_i^{1+(\alpha/2)}} \int s ds,$$
$$\frac{2}{|f_i'|^{1/2}} = \frac{2s^2 + 2A}{3h_i^{1+(\alpha/2)}}.$$

Since $h_2 < 1$, we expect $f_i'(s) < 0$ and we may take care of the modulus signs to solve for $f_i'(s)$ as

$$f_i'(s) = -\frac{9h_i^{\alpha+2}}{\left(s^2 + A_i\right)^2}, \tag{17}$$

for some constant of integration, A_i, which cannot be determined from the given condition on $f_i(s)$; namely, $f_i(s) \to 0$ as $|s| \to \infty$. Taking $|s| \to \infty$, (17) gives $f_i'(s) \to 0$ and demonstrates self-consistency with the initial assumption on $(F_i^{\text{lin}})'$.

To integrate further we need to consider cases for different signs of A_i.

- If $A_i > 0$, integrating (17) gives

$$\begin{aligned} f_i(s) &= -\frac{9h_i^{\alpha+2}}{A_i^2} \int \left(\left(\frac{s}{A_i} \right)^2 + 1 \right)^{-2} ds \\ &= -\frac{9h_i^{\alpha+2}}{2A_i^{3/2}} \left\{ \frac{A_i^{1/2} s}{s^2 + A_i} + \arctan\left(\frac{s}{A_i^{1/2}} \right) + B_i \right\}. \end{aligned} \tag{18}$$

  But $f_i(s) \to 0$ as $|s| \to \infty$ for $i = 1, 2$ implies

$$B_1 = \frac{\pi}{2}, \text{ and } \; B_2 = -\frac{\pi}{2}.$$

  Hence, equations (17) and (18) give rise to the following equations for $F_i^{\text{lin}}(s)$ and its derivative when $A_i > 0$

$$\left(F_i^{\text{lin}}(s)\right)' = -\frac{9h_i^{\alpha+2}}{\left(s^2 + A_i\right)^2}, \tag{19}$$

$$F_i^{\text{lin}}(s) = h_i - \frac{9h_i^{\alpha+2}}{2A_i^{3/2}} \left\{ \frac{A_i^{1/2} s}{s^2 + A_i} + \arctan\left(\frac{s}{A_i^{1/2}} \right) + \delta_i \frac{\pi}{2} \right\}, \tag{20}$$

  where

$$\delta_i = \begin{cases} 1 & \text{for } \; i = 1 \\ -1 & \text{for } \; i = 2. \end{cases}$$

- If $A_i < 0$, integrating (17) gives

$$f(s) = -\frac{9h_i^{\alpha+2}}{|A_i|^2}\int\left(\left(\frac{s}{|A_i|^{1/2}}\right)^2 - 1\right)^{-2} ds$$
$$= -\frac{9h_i^{\alpha+2}}{2|A_i|^{3/2}}\left\{\left(\frac{1}{2}\right)\ln\left|\frac{s+|A_i|^{1/2}}{s-|A_i|^{1/2}}\right| - \frac{|A_i|^{1/2}s}{s^2+|A_i|} + C_i\right\}. \quad (21)$$

But $f_i(s) \to 0$ as $|s| \to \infty$ for $i = 1, 2$ implies $C_i = 0$. Hence, equations (17) and (21) give rise to the following equations for $F_i^{\text{lin}}(s)$ and its derivative when $A_i < 0$

$$\left(F_i^{\text{lin}}(s)\right)' = -\frac{9h_i^{\alpha+2}}{\left(s^2+A_i\right)^2}, \quad (22)$$

$$F_i^{\text{lin}}(s) = h - \frac{9h_i^{\alpha+2}}{2|A_i|^{3/2}}\left\{\left(\frac{1}{2}\right)\ln\left|\frac{s+|A_i|^{1/2}}{s-|A_i|^{1/2}}\right| - \frac{|A_i|^{1/2}s}{s^2+|A_i|}\right\}. \quad (23)$$

- If $A_i = 0$, equation (17) is more simple to integrate; the constant of integration is zero and we have

$$\left(F_i^{\text{lin}}(s)\right)' = -\frac{9h_i^{\alpha+2}}{s^4}, \quad (24)$$

$$F_i^{\text{lin}}(s) = h_i + \frac{3h_i^{\alpha+2}}{s^3}. \quad (25)$$

Here it is understood that these equations give an approximate solution to (12) as $s \to \pm\infty$, and at each of the limits the constants A_i will, in general, not be equal. It is no surprise that the A_i cannot be determined since we are solving a second order differential equation for f_i, but there is only one boundary condition on each f_i. It is clear that A_1 will depend on h_2 since a change in h_2 will require a change in gradient on the left (and hence a different A_1). We need to find constants A_1 and A_2 such that when the non-linear 'middle section' is solved, the solution matches with the boundary conditions (provided by A_1 and A_2) at both ends of the solution.

3.3 Numerical solutions of (12) for the wet dam-break

Suppose we take $s_{\text{left}} < 0$ and $s_{\text{right}} > 0$ as the points where we establish boundary conditions for $F(s)$ using the solutions (19)-(25). We can find the constants A_1 and A_2 numerically using the following steps (see appendix B.1 for the MATLAB code):

- Guess A_1 and use equations (19)-(25) (depending on the choice of the guess) to determine $F_1^{\text{lin}}(s_{\text{left}})$ and $\left(F_1^{\text{lin}}(s_{\text{left}})\right)'$.
- Use ode45 to solve (12) on $[s_{\text{left}}, s_{\text{right}}]$ with $F_1^{\text{lin}}(s_{\text{left}})$ and $\left(F_1^{\text{lin}}(s_{\text{left}})\right)'$ as the boundary conditions.
- Use ode45's solution to find $F(s_{\text{right}})$ and $F'(s_{\text{right}})$ based on the guess of A_1.
- Use equation (17) to find the required A_2 such that

$$\left(F_2^{\text{lin}}(s_{\text{right}})\right)' = F'(s_{\text{right}}).$$

- Using the obtained value for A_2, evaluate $F_2^{\text{lin}}(s_{\text{right}})$.
- Find the difference of this with $F(s_{\text{right}})$ obtained earlier from solving (12) on $[s_{\text{left}}, s_{\text{right}}]$ with the guessed A_1, i.e. calculate

$$F_{\text{difference}} = F_2^{\text{lin}}(s_{\text{right}}) - F(s_{\text{right}}).$$

- Repeat the above steps with another guess for A_1. Then, using the secant method (see appendix A.2), find A_1 such that

$$|F_{\text{difference}}(A_1)| < \delta,$$

where δ is some specified error tolerance.

Taking $[s_{\text{left}}, s_{\text{right}}] = [-10, 10]$ and $h_2 = 0.2$, the above procedure under various α values yields solutions like those in figures 2 and 3. Here, all solutions were solved and plotted using the MATLAB code in B.1 and care was taken over the choice of s_{left}, s_{right}, δ and ode45's 'options' to ensure an accurate solution.

The Manning plot is a similar shape to the Chézy plot but 'squeezed' inwards (although not perfectly axis-symmetrically). Hence, in this case, Manning friction generally reduces the speed at which the height profile expands and has a stronger effect than Chézy friction. This is to be expected since the the friction term is proportional to $h^{-\alpha}$, thus a larger α provides a more dominant friction term.

Evaluation of (23) determines that if $A_1 < -s_{\text{left}}^2 < 0$, then $F(s_{\text{left}}) > 1$, which is inconsistent with the assumption that $f'(s) < 0$ everywhere for $h_2 < 1$. It is possible for A_1 to take a smaller negative value however.

Table 1 gives the values of A_1 to two decimal places for various h_2 with Chézy friction and $s_{\text{right}} = -s_{\text{left}} = 10$. As expected, A_1 decreases for h_2 decreasing. This reflects the steeper gradient needed at s_{left} required to meet a smaller h_2 at s_{right}.

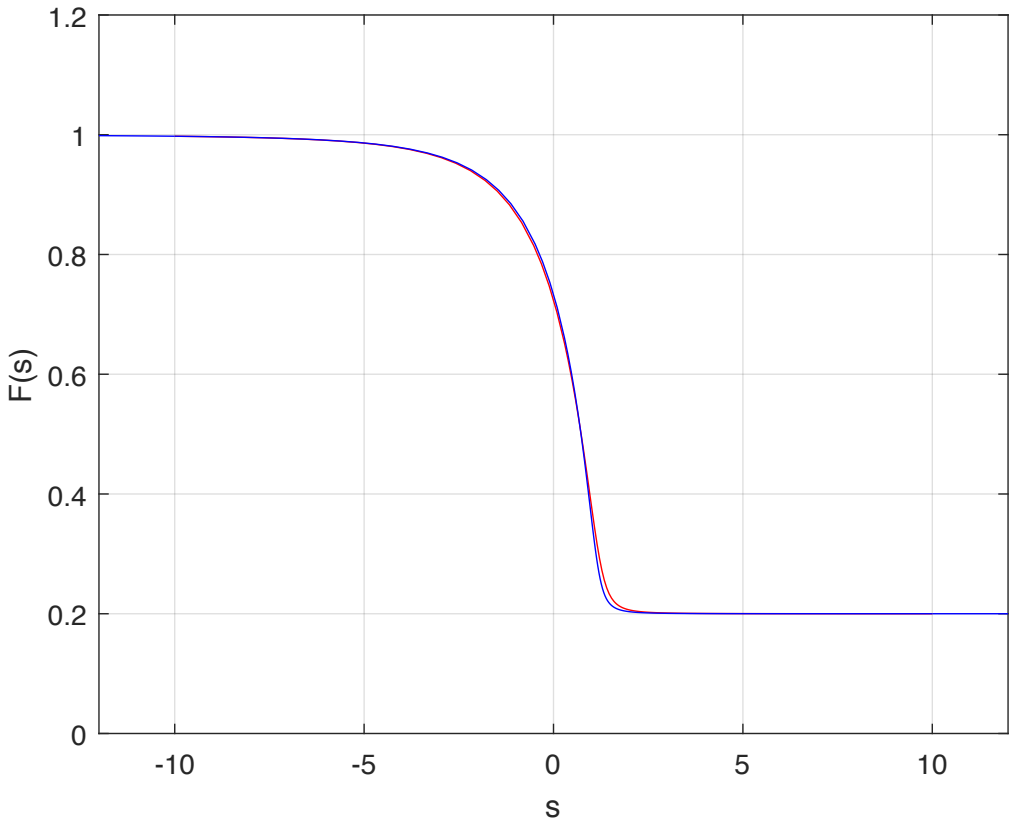

Figure 2: A plot of s against $F(s)$ for $h_2 = 0.2$ under Chézy friction (red) and Manning friction (blue).

It appears that A_1 is converging as $h_2 \to 0$. This is a fair conclusion to draw since, as mentioned above, $A_1 < s_{\text{left}}$ is not permitted. Thus since s_{left} is finite and A_1 is monotonic with respect to h_2 (which is intuitively obvious), A_1 must converge. Fig. 4 gives a visual display of this convergence as $h_2 \to 0$.

h_2	0.05	0.1	0.15	0.2	0.25	0.3	0.35	0.4	0.45	0.5
A_1	14.80	14.86	14.93	15.02	15.13	15.26	15.42	15.62	15.86	16.17

Table 1: Table showing the relationship of A_1 values with h_2 (under Chézy friction).

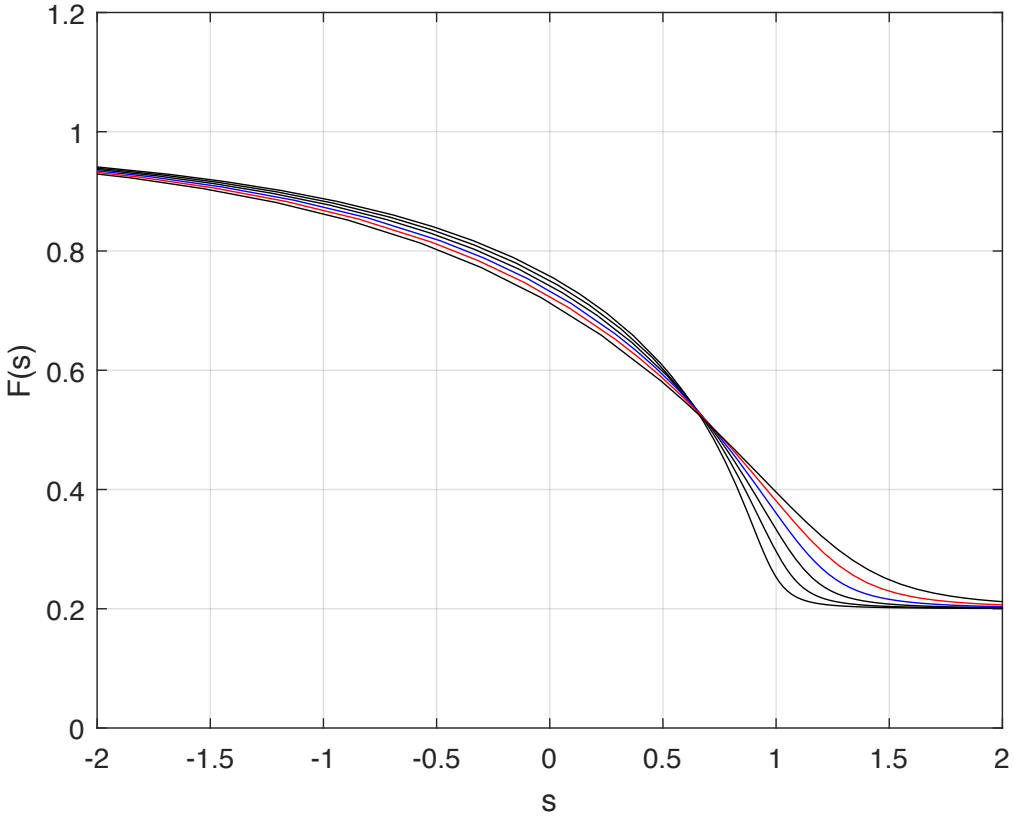

Figure 3: A rescaled version of figure 2 with the addition of more α cases for comparison. In the red to blue direction the cases are from $\alpha = 2/3$ to $\alpha = 7/3$ increasing in increments of $1/3$, behaving as expected.

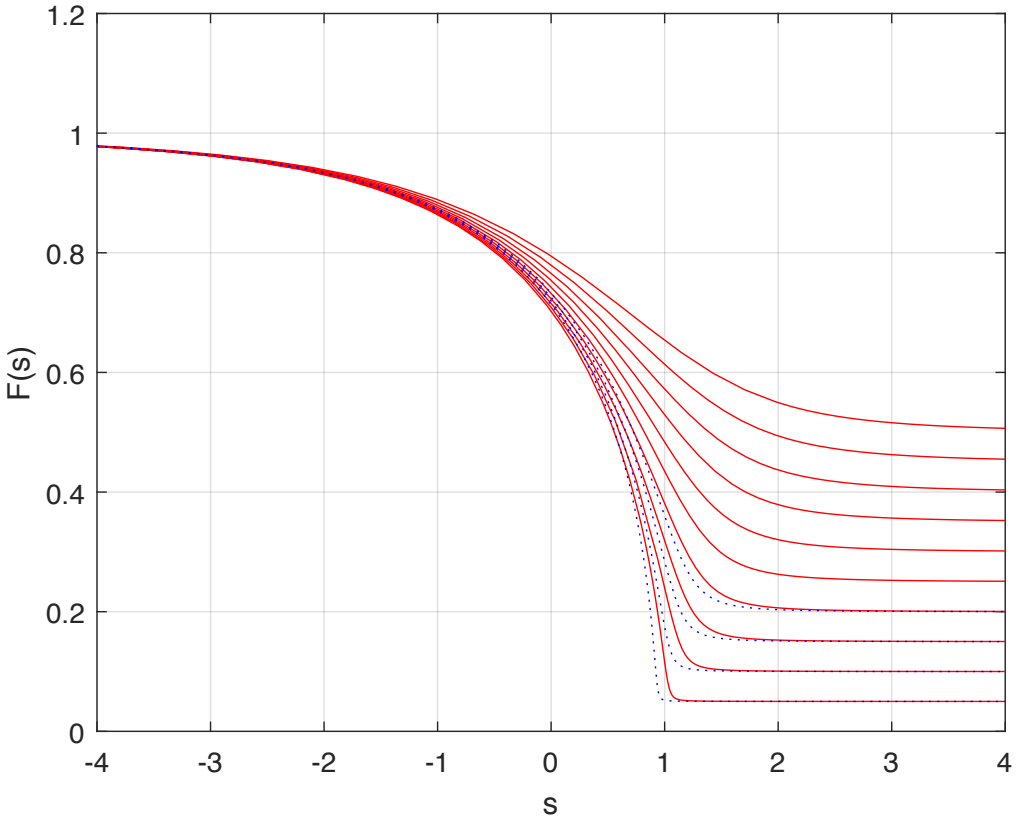

Figure 4: A plot comparing various solutions for Chézy friction with h_2 ranging from 0.05 to 0.5 in increments of 0.05. For $h_2 = 0.05$ to $h_2 = 0.2$, Manning friction is also plotted (dashed blue) for means of comparing the 'turning point' as $h_2 \to 0$.

4 Dry Dam-Break Problem

4.1 Set up and initial conditions

The above method breaks down for $h_2 = 0$ since $F(s) = 0$ is a singularity of (12). We devise an alternative method for solving the problem when $h_2 = 0$ by considering the solution near the leading edge of the fluid. The boundary conditions for $F(s)$ in this problem are the same as in the general dam-break problem with h_2 set to zero. That is

$$\begin{cases} F(s) \to 1 & \text{as} \quad s \to -\infty \\ F(s) \to 0 & \text{as} \quad s \to \infty. \end{cases}$$

However, since we expect there to exist some $\tilde{x}(t)$ such that $h(x,t) = 0$ for all $x > \tilde{x}(t)$, we assume $F(s) = 0$ for large enough s, i.e. for all s larger than some constant s_0. Hence, the conditions can be reformed as

$$\begin{cases} F(s) \to 1 & \text{as} \quad s \to -\infty \\ F(s) = 0 & \text{for} \quad s > s_0, \end{cases} \tag{26}$$

where s_0 is an unknown to be found as part of the solution.

4.2 Solution near the wave front

Our aim is to solve (12) subject to boundary conditions (26). Since $F(s_0)$ is a singularity of (12), we seek a solution near the head by forming the ansatz

$$F^{\text{head}}(s) = C\left(s_0 - s\right)^{\beta}, \tag{27}$$

for constants C and β. Letting $\epsilon = s_0 - s$, we have

$$\begin{aligned} F^{\text{head}}(s) &= C\epsilon^{\beta}, \\ \left(F^{\text{head}}(s)\right)' &= -C\beta\epsilon^{\beta-1}, \\ \left(F^{\text{head}}(s)\right)'' &= C\beta\left(\beta-1\right)\epsilon^{\beta-2}, \end{aligned}$$

which upon substitution into (12) yields

$$C\beta\left(\beta-1\right)\epsilon^{\beta-2} = \frac{4s}{3}\frac{C\beta\epsilon^{\beta-1}|C\beta\epsilon^{\beta-1}|^{1/2}}{\left(C\epsilon^{\beta}\right)^{\frac{\alpha}{2}+1}} - (\alpha+2)\frac{\left(C\beta\epsilon^{\beta-1}\right)^2}{C\epsilon^{\beta}}. \tag{28}$$

Equating the powers of ϵ we see that we must have

$$\beta - 2 = -\left(\frac{\alpha-1}{2}\right)\beta - \frac{3}{2},$$

and hence

$$\beta = \frac{1}{\alpha+1} = \begin{cases} 1/2 & \text{when } \alpha = 1 \quad \text{(Chézy)} \\ 3/7 & \text{when } \alpha = 4/3 \quad \text{(Manning).} \end{cases} \tag{29}$$

Substituting β into equation (28) finds for C the equation

$$C\left(\frac{1}{\alpha+1}\right)\left(\frac{-\alpha}{\alpha+1}\right) = \frac{4s}{3}C^{(1-\alpha)/2}\left(\frac{1}{\alpha+1}\right)^{3/2} - (\alpha+2)C\left(\frac{1}{\alpha+1}\right)^{2}.$$

Rearranging finds

$$C = \left((\alpha+1)\,\frac{4s_0^2}{9}\right)^{1/(\alpha+1)}. \tag{30}$$

Finally, equations (27), (29) and (30) combine to give the solution near the head as

$$F^{\text{head}}(s) = \left(\frac{4s_0^2}{9}\,(\alpha+1)\,(s_0-s)\right)^{1/(\alpha+1)}. \tag{31}$$

In particular, if

- $\alpha = 1$ (Chézy friction), then

$$F^{\text{head}}(s) = \frac{2\sqrt{2}}{3}s_0\,(s_0-s)^{1/2}.$$

- $\alpha = 4/3$ (Manning friction), then

$$F^{\text{head}}(s) = \left(\frac{2\sqrt{7}}{3\sqrt{3}}s_0\right)^{6/7}(s_0-s)^{3/7}.$$

Equation (31) gives the leading order profile of the height near the front edge of the flow. Furthermore, (31) gives the gradient of the leading order profile of the height near the front edge. Both of these will be used below to solve the dry dam-break numerically. Explicitly for reference

$$\left(F^{\text{head}}(s)\right)' = \frac{1}{\alpha+1}\left(\frac{4s_0^2}{9}\,(\alpha+1)\,(s_0-s)\right)^{-\alpha/(\alpha+1)}. \tag{32}$$

4.3 Numerical solutions of (12) for the dry dam-break

If we consider solving (12) on the domain $[s_{\text{left}}, s_0-\epsilon]$ for some chosen numerical parameters $-s_{\text{left}} \gg 1$, $\epsilon \ll 1$ and a guessed value of $s_0 > 0$, then we find ourselves in a similar position to the wet dam-break problem. Similar in the sense that from (19)-(25) and (31)-(32) we have the dynamics

for $F_1^{\text{lin}}(s_{\text{left}})$ and $F^{\text{head}}(s_0 - \epsilon)$ so we can establish boundary conditions at both ends of the domain $[s_{\text{left}}, s_0 - \epsilon]$.

The problem is not identical to numerically solving (12) for the wet dam-break though since the upper edge of the domain is now free to move (since s_0 is an unknown that we are solving for). We can overcome this and find s_0 by using a similar approach to that of finding A_1 in the wet dam-break problem. Since we are interested in finding s_0, however, we will work first from the boundary conditions on the right hand side. That is, consider the height and gradient at the upper edge of the domain for some s_0 and use these to solve (12). Then, comparing the solution with the linearised approximations for height and gradient at the lower end of the domain, adjust s_0 accordingly. In full,

- Guess some sensible s_0 value and use (31) and (32) to calculate $F^{\text{head}}(s_0 - \epsilon)$ and $\left(F^{\text{head}}(s_0 - \epsilon)\right)'$.
- Use these with ode45 to solve (12) on $[s_{\text{left}}, s_0 - \epsilon]$.
- Find $F(s_{\text{left}})$ and $F'(s_{\text{left}})$ from ode45's solution and use $F'(s_{\text{left}})$ to determine the constant, A_1, for the linearised solution at large negative s values.
- From the obtained A_1 value, calculate $F_1^{\text{lin}}(s_{\text{left}})$ using (19)-(25).
- Compare $F_1^{\text{lin}}(s_{\text{left}})$ with $F(s_{\text{left}})$ obtained from ode45's solution under the guess for s_0, i.e. calculate

$$\tilde{F}_{\text{difference}}(s_0) = F_1^{\text{lin}}(s_{\text{left}}) - F(s_{\text{left}}).$$

- Repeat the above steps with another guess for s_0. Then using the secant method (see appendix A.2), find s_0 such that

$$|\tilde{F}_{\text{difference}}(s_0)| < \delta,$$

  where δ is some specified error tolerance.

Evaluating the position of the sharp turn in figure 4 as $h_2 \to 0$ indicates a 'sensible guess' for s_0 is somewhere near to 1.

The value for s_0 is found (again, using the MATLAB code in appendix B.1 and considering the appropriate error tolerances in the numerical method) as:

$$\begin{array}{ll} \text{for Chézy friction,} & s_0 = 0.9086... \\ \text{for Manning friction,} & s_0 = 0.8306... \end{array}$$

Figure 5 shows the plots in both cases. Table 2 displays s_0 values for a wider range of α and figure 7 has these plotted on a scatter graph.

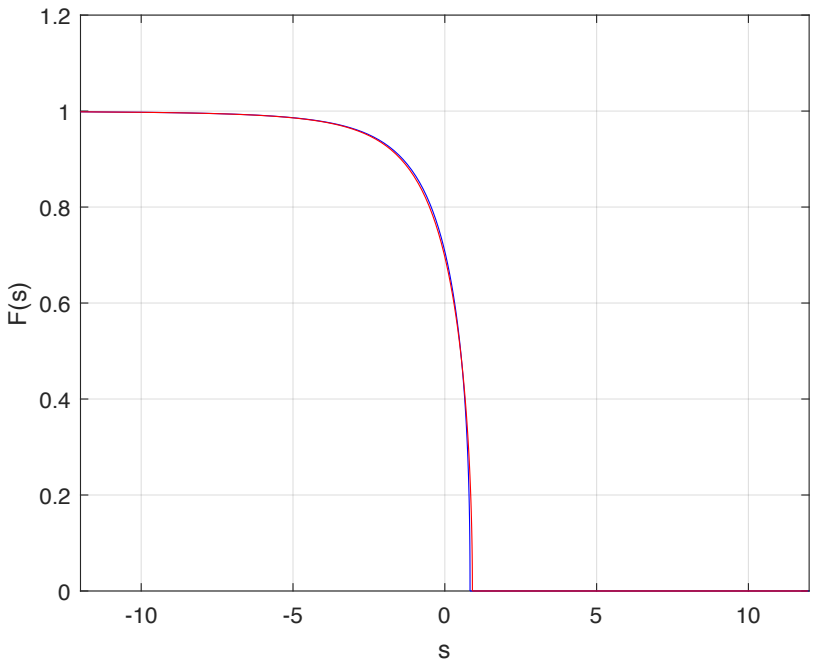

Figure 5: A plot of s against $F(s)$ for the dry dam-break under Chézy friction (red) and Manning friction (blue).

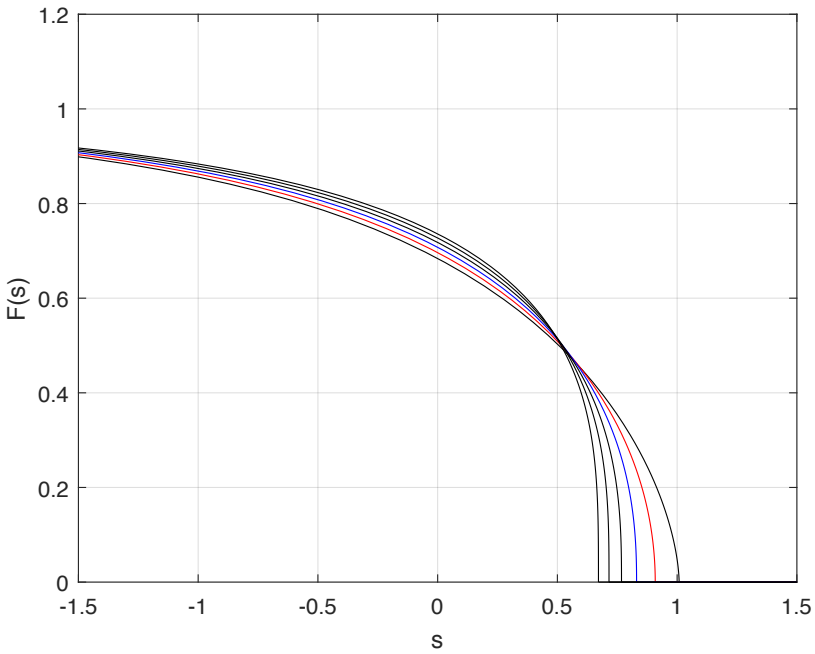

Figure 6: A rescaled version of figure 5 with the addition of more α cases. In the red to blue direction the cases are from $\alpha = 2/3$ to $\alpha = 7/3$ increasing in increments of $1/3$, behaving as expected.

α	4/6	5/6	6/6	7/6	8/6	9/6	10/6	11/6	12/6	13/6	14/6
s_0	1.083	0.9551	0.9086	0.8674	0.8306	0.7976	0.7677	0.7404	0.7155	0.6926	0.6714

Table 2: Table showing the relationship of α and s_0

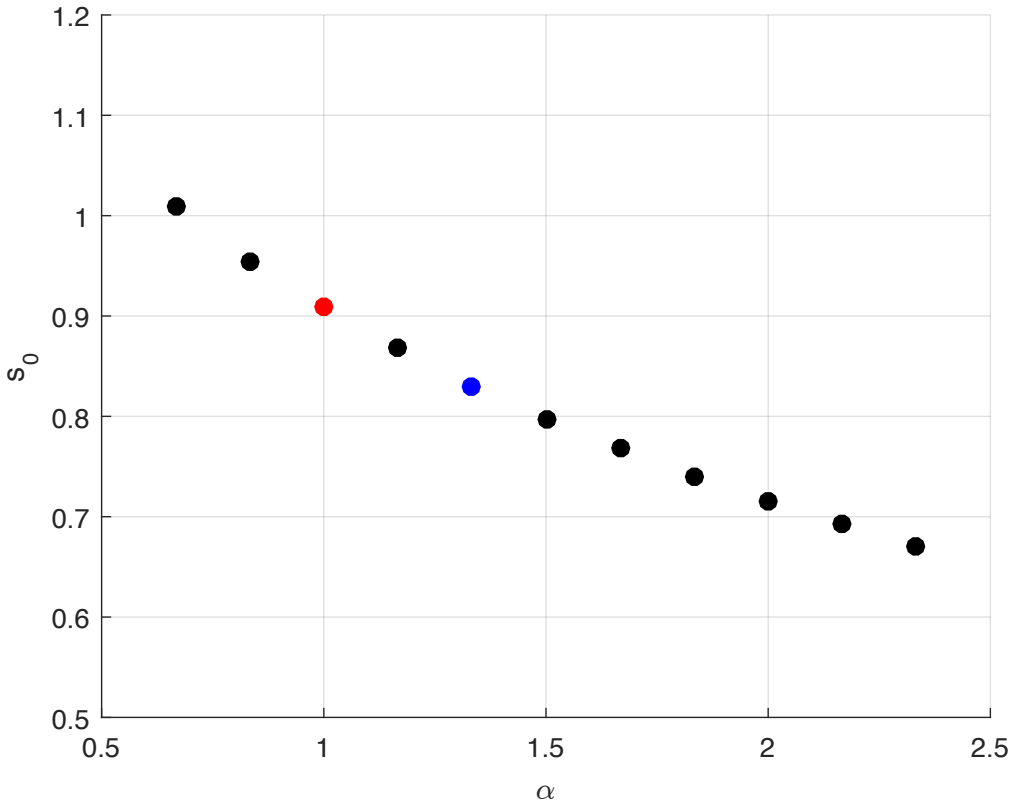

Figure 7: A scatter plot displaying the relationship between α and s_0. Here, α has been chosen to increase in increments of 1/6 and the particular cases of Chézy and Manning are highlighted in red and blue respectively.

Recalling $s = xt^{-2/3}$, the leading front of the fluid at time t, according to the model, has position

$$x_f = s_0 t^{\frac{2}{3}}, \tag{33}$$

and velocity

$$v_f = \frac{2s_0}{3} t^{-\frac{1}{3}}. \tag{34}$$

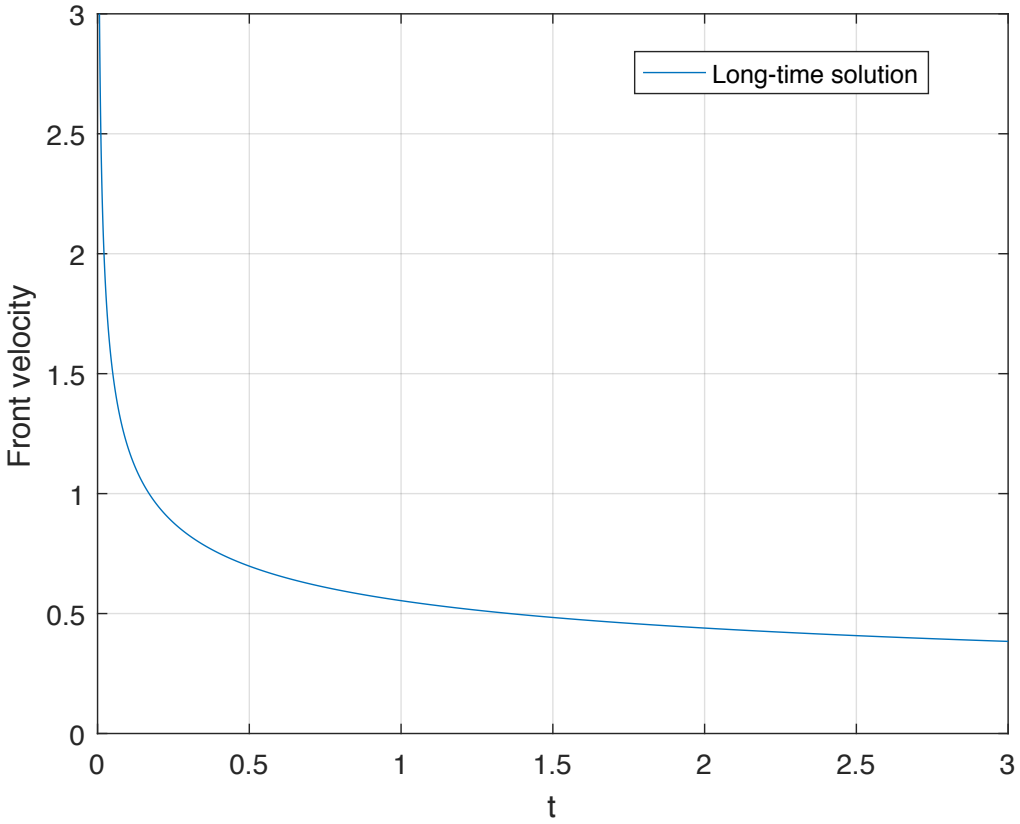

Figure 8: A plot for the front velocity modelled by (34).

5 Front Velocity at Small Times

5.1 Whitham's solution for Chézy friction

The solution for v_f given by (34) is only derived for $t \to \infty$. Indeed, as $t \to 0$, $v_f \to \infty$ which is clearly unrealistic. The aim of this chapter is to find v_f at small times. It is possible to seek solutions by expanding about a parameter $R = 1/r^2$ in (7) and (8) to solve for a large r (and hence find the small time solution). This was attempted by Dressler (1952) [2] for Chézy friction, however the method was found to break down near the front where h is small (since the friction term is no longer simply a small perturbation in this region).

Whitham (1955) [3] derived a more accurate approximate solution for x_f at small times under Chézy friction by considering the tip region at the head of the flow as a 'boundary layer' at small times. In the derivation, friction is neglected away from the tip region and the Ritter (1892) [1] solution for the frictionless shallow water equations (see appendix A.3) is presumed away from the tip region; for reference, Ritter's solution (in dimensionless variables) reads

$$u(x,t) = \begin{cases} 0, & \text{if } x < -t \\ \dfrac{2}{3}\left(\dfrac{x}{t} + 1\right), & \text{if } -t < x < 2t \\ 0, & \text{if } x > 2t \end{cases} \tag{35}$$

$$h(x,t) = \begin{cases} 1, & \text{if } x < -t \\ \dfrac{1}{9}\left(\dfrac{x}{t} - 2\right)^2, & \text{if } -t < x < 2t \\ 0, & \text{if } x > 2t. \end{cases} \tag{36}$$

Let $[\xi, x_f]$ be the tip region, $M(t)$ and $P(t)$ be the total mass and momentum respectively in the tip region, $U(t) = u(\xi, t)$, $H(t) = h(\xi, t)$ and fluid density ρ taken without loss of generality as 1. The total rate of change of mass in the tip region is found as the flux of mass over the back of the tip region $x = \xi(t)$, hence

$$\frac{dM}{dt} = h(\xi,t)\left(u(\xi,t) - \frac{d\xi}{dt}\right) = H\left(U - \frac{d\xi}{dt}\right). \tag{37}$$

Similarly, the rate of momentum flow across $x = \xi(t)$ is UM_t, giving

$$\frac{dP}{dt} = UH\left(U - \frac{d\xi}{dt}\right) + F, \tag{38}$$

where F is the horizontal force on the tip region.

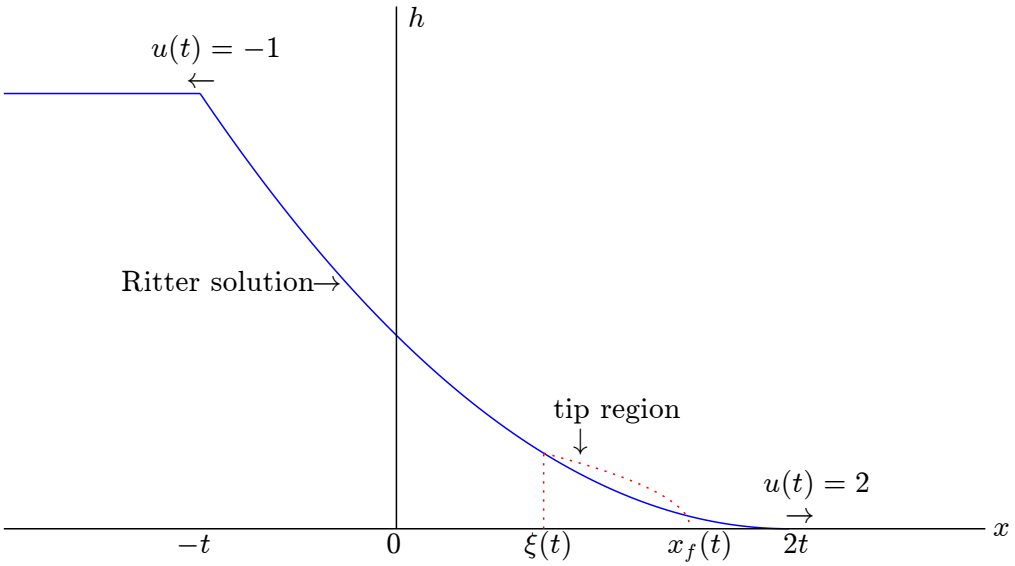

Figure 9: Whitham's general set up.

Whitham finds the horizontal pressure on the tip by arguing that the horizontal component of atmospheric pressure acting on the free surface of the tip must be balanced by the hydrostatic pressure over $x = \xi$, i.e $\int H dH$. Thus, as a result

$$F = \frac{1}{2}H^2 + \text{resistance force from friction.}$$

Equation (8) gives the resistance from friction on the tip as

$$\text{resistance force from friction} = -\int_{\xi}^{x_f} \frac{hu^2}{h^{\alpha}} dx = -\int_{\xi}^{x_f} \frac{u^2}{h^{\alpha-1}} dx, \tag{39}$$

and hence,

$$F = \frac{1}{2}H^2 - \int_{\xi}^{x_f} \frac{u^2}{h^{\alpha-1}} dx. \tag{40}$$

We point out that this result for P_t can be derived purely from the frictional shallow water equations. If we multiply the momentum equation (8) by h to give

$$hu_t + huu_x + hh_x = -\frac{u^2}{h^{\alpha-1}},$$

and the mass conservation equation (7) by u to give

$$uh_t + u\left(hu\right)_x = 0,$$

then we can add the results to find the conservational momentum equation as

$$\left(uh\right)_t + \left(u^2 h + \frac{1}{2}h^2\right)_x = -\frac{u^2}{h^{\alpha-1}}. \tag{41}$$

Integrating with respect to x over the tip region $[\xi(t), x_f(t)]$, (41) becomes

$$\int_{\xi(t)}^{x_f(t)} (uh)_t \, dx + [u^2 h + \frac{1}{2}h^2]_{\xi}^{x_f} = -\int_{\xi}^{x_f} \frac{u^2}{h^{\alpha-1}} dx,$$

so using $h(x_f(t), t) = 0$ and $h(\xi(t), t) = H$ we have

$$\int_{\xi(t)}^{x_f(t)} (uh)_t \, dx = U^2 H + \frac{1}{2}H^2 - \int_{\xi}^{x_f} \frac{u^2}{h^{\alpha-1}} dx. \tag{42}$$

Leibniz's rule for differentiation under the integral sign gives

$$\begin{aligned}
\frac{dP}{dt} &= \frac{d}{dt}\int_{\xi(t)}^{x_f(t)} (uh)\, dx \\
&= \int_{\xi(t)}^{x_f(t)} (uh)_t \, dx + u(x_f(t), t)h(x_f(t), t)\frac{dx_f}{dt} - u(\xi(t), t)h(\xi(t), t)\frac{d\xi}{dt} \\
&= \int_{\xi(t)}^{x_f(t)} (uh)_t \, dx - UH\frac{d\xi}{dt}. \qquad (43)
\end{aligned}$$

Combining (42) and (43) gives the same result as above. In full

$$\frac{dP}{dt} = UH\left(U - \frac{d\xi}{dt}\right) + \frac{1}{2}H^2 - \int_{\xi}^{x_f} \frac{u^2}{h^{\alpha-1}} dx. \tag{44}$$

For Chézy friction, $\alpha = 1$ eliminates h in the integrand of (39). Under the assumption that $u = U(t) = \dot{x}_f(t)$ throughout the tip region, Whitham could then integrate the resistance term successfully as

$$F = \frac{1}{2}H^2 - \dot{x}_f^2 \, (x_f - \xi) \, dx. \tag{45}$$

Another consequence of assuming the velocity profile $\dot{x}_f$ throughout the tip region is

$$\frac{dP(t)}{dt} = \frac{d}{dt}\left(\dot{x}_f M\right) = \dot{x}_f \frac{dM}{dt} + \ddot{x}_f M, \tag{46}$$

which leads Whitham to combine (37), (38) and (45) to imply

$$\ddot{x}_f M = \frac{1}{2}H^2 - \dot{x}_f^2 \int_{\xi}^{x_f} dx = \frac{1}{2}H^2 - \dot{x}_f^2 \left(x_f - \xi\right). \tag{47}$$

From the Ritter solution and using $u(\xi, t) = \dot{x}_f$, equations for ξ and H in terms of $\dot{x}_f$ are found. Explicitly,

$$\xi(t) = \left(\frac{3\dot{x}_f}{2} - 1\right) t, \tag{48}$$

$$H(t) = \left(1 - \frac{\dot{x}_f}{2}\right)^2. \tag{49}$$

Also, M can be found using the Ritter solution since M must be the same as the mass in front of $x = \xi$ with friction neglected. Hence, sustitution of (36) for h and (48) for ξ finds

$$\begin{aligned} M(t) = \int_{\xi}^{x_f} h(x,t)dx &= \int_{\xi}^{2t} \frac{1}{9}\left(2 - \frac{x}{t}\right)^2 dx \\ &= \frac{1}{27}\left(2 - \frac{\xi}{t}\right)^3 t \\ &= \left(1 - \frac{\dot{x}_f}{2}\right)^3 t. \end{aligned} \tag{50}$$

Finally, rewriting (47) purely in terms of x_f and its derivatives and rearranging yields Whitham's equation for the front position as

$$2\ddot{x}_f\left(1 - \frac{\dot{x}_f}{2}\right)^3 t = \left(1 - \frac{\dot{x}_f}{2}\right)^4 - 2\dot{x}_f^2\left\{x_f - t\left(\frac{3\dot{x}_f}{2} - 1\right)\right\}. \tag{51}$$

5.2 Adjusting Whitham's solution for general friction

For Manning friction, $\alpha = 4/3$ and $h(x,t)$ is not eliminated in the integral term of (40). In fact, in general, for $\alpha \neq 1$, (44) has an integral term that is not immediately straightforward to calculate (since in such cases the integrand has explicit x dependence through $h(x,t)$).

To proceed we seek a power series for $u(x,t)$ and $h(x,t)$ about $x = x_f$ and substitute into (7) and (8). By definition $u(x_f,t) = \dot{x}_f$, so the first term of the $u(x,t)$ series must be $\dot{x}_f$. Let the first term of the $h(x,t)$ series be denoted by $\tilde{h}$, say. Now evaluating the momentum equation (8) at the first order finds

$$\tilde{h}_x = -\frac{\dot{x}_f^2}{\tilde{h}^\alpha}.$$

Hence

$$\dot{x}_f^2 = -\tilde{h}^\alpha \tilde{h}_x = -\frac{d}{dx}\left(\frac{\tilde{h}^{\alpha+1}}{\alpha+1}\right),$$

which may be integrated with respect to x as

$$x\dot{x}_f^2 = -\frac{\tilde{h}^{\alpha+1}}{\alpha+1} + A(t),$$

for some function A of t only (constant in x). Considering $h(x_f,t) = 0$ we conclude $A(t) = x_f\dot{x}_f^2$ and

$$(x - x_f)\,\dot{x}_f^2 = -\frac{\tilde{h}^{\alpha+1}}{\alpha+1}.$$

Rearranging for $\tilde{h}(x,t)$ gives

$$\tilde{h}(x,t) = \left((\alpha+1)\,\dot{x}_f^2\right)^{\frac{1}{\alpha+1}} (x_f - x)^{\frac{1}{\alpha+1}} = h_0\,(x_f - x)^{\frac{1}{\alpha+1}}\,,$$

where

$$h_0(t) = \left((\alpha+1)\,\dot{x}_f^2\right)^{\frac{1}{\alpha+1}}\,, \tag{52}$$

has been introduced for notational brevity.

Having found the first term for both power series, we seek solutions for $u(x,t)$ and $h(x,t)$ of the form

$$u(x,t) = \dot{x}_f + u_p(t)\,(x_f - x)^p + \cdots\,, \tag{53}$$

$$h(x,t) = h_0(t)\,(x_f - x)^{\frac{1}{\alpha+1}} + h_q(t)\,(x_f - x)^q + \cdots\,, \tag{54}$$

for some numbers $p > 0$, $q > 1/(\alpha+1)$ to be found such that $u_p \neq 0$, $h_q \neq 0$. Substituting (53) and (54) into (7) we have (after cancellation of some terms)

$$\begin{aligned} 0 = {} & \dot{h}_0\,(x_f - x)^{\frac{1}{\alpha+1}} + \dot{h}_1\,(x_f - x)^q + \cdots \\ & - \left\{u_1\,(x_f - x)^p + \cdots\right\}\left\{\frac{h_0}{\alpha+1}\,(x_f - x)^{\frac{1}{\alpha+1}-1} + \cdots\right\} \\ & - \left\{\frac{u_1}{p}\,(x_f - x)^{p-1} + \cdots\right\}\left\{h_0\,(x_f - x)^{\frac{1}{\alpha+1}} + \cdots\right\}, \end{aligned} \tag{55}$$

and clearly $p = 1$ is necessary. Equating the $(x_f - x)^{1/(\alpha+1)}$ terms we find

$$\dot{h}_0 - \frac{h_0 u_1}{\alpha+1} - h_0 u_1 = 0,$$

which yields

$$u_1(t) = \left(\frac{\alpha+1}{\alpha+2}\right)\frac{\dot{h}_0}{h_0}.$$

Substitution of (52) finds

$$u_1(t) = \left(\frac{2}{\alpha+2}\right)\frac{\ddot{x}_f}{\dot{x}_f}.$$

To determine $h_q(t)$ we need to use (8). Noting the $h^{-\alpha}$ term, we make use of the general result from Maclaurin series that for small ϵ and constants A, B, C and D we have

$$\left(A\epsilon^B + C\epsilon^D\right)^{-\alpha} = A^{-\alpha}\epsilon^{-\alpha B} - \frac{\alpha C}{A^{\alpha+1}}\epsilon^{D-(1+\alpha)B} - \cdots\,. \tag{56}$$

Substituting (53) and (54) into (8) and using (56) gives (after cancellation of some terms)

$$\begin{aligned}0 &= \ddot{x}_f + \dot{u}_1(t)\,(x_f - x) + \cdots - (u_1\,(x_f - x) + \cdots)\,(u_1 + \cdots) \\ &\quad - (\alpha+1)\,h_0\,(x_f - x)^{\frac{1}{\alpha+1}-1} - q h_1\,(x_f - x)^{q-1} - \cdots \\ &\quad + \left\{\dot{x}_f^2 + \cdots\right\}\left\{h_0^{-\alpha}\,(x_f - x)^{\frac{1}{\alpha+1}-1} - \frac{\alpha h_1}{h_0^{\alpha+1}}\,(x_f - x)^{q-1} - \cdots\right\}. \end{aligned} \tag{57}$$

Equating the leading order terms in (57) confirms h_0 since that was how we derived h_0 in the first instance. At the next order in $x_f - x$ it is necessary to take $q = 1$ to balance the acceleration term. Indeed we find

$$\ddot{x}_f - \frac{\alpha h_1 \dot{x}_f^2}{h_0^{\alpha+1}} = 0,$$

and using (52) we have

$$h_1(t) = \left(\frac{\alpha+1}{2\alpha+1}\right)\ddot{x}_f.$$

Thus the expansions for $u(x,t)$ and $h(x,t)$ are

$$u(x,t) = \dot{x}_f + \left(\frac{2}{\alpha+2}\right)\frac{\ddot{x}_f}{\dot{x}_f}\,(x_f - x) + \cdots \tag{58}$$

$$h(x,t) = \left((\alpha+1)\,\dot{x}_f^2\right)^{\frac{1}{\alpha+1}}(x_f - x)^{\frac{1}{\alpha+1}} + \left(\frac{\alpha+1}{2\alpha+1}\right)\ddot{x}_f\,(x_f - x) + \cdots. \tag{59}$$

We are now in a position to find the resistance component (the final term) of (40). Using the expansions (58) and (59) gives

$$\begin{aligned} u^2 h^{1-\alpha} &= \left\{\dot{x}_f^2 + 2u_1\dot{x}_f\,(x_f - x) + \cdots\right\} \\ &\qquad \left\{h_0^{1-\alpha}\,(x_f - x)^{\frac{1-\alpha}{1+\alpha}} + (1-\alpha)\,\frac{h_1}{h_0^{\alpha}}\,(x_f - x)^{\frac{1}{\alpha+1}} + \cdots\right\} \\ &= \dot{x}_f^2\left\{h_0^{1-\alpha}\,(x_f - x)^{\frac{1-\alpha}{1+\alpha}} + (1-\alpha)\,\frac{h_1}{h_0^{\alpha}}\,(x_f - x)^{\frac{1}{\alpha+1}} + \cdots\right\} \\ &\quad + 2u_1\dot{x}_f\left\{h_0^{1-\alpha}\,(x_f - x)^{\frac{2}{1+\alpha}} + \cdots\right\}. \end{aligned}$$

Hence, we calculate the resistance integral as

$$\begin{aligned}\int_{\xi}^{x_f}\frac{u^2}{h^{\alpha-1}}dx &= \dot{x}_f^2 h_0^{1-\alpha}\left(\frac{\alpha+1}{2}\right)(x_f - \xi)^{\frac{2}{\alpha+1}} + \cdots \\ &= \frac{1}{2}\left((\alpha+1)\,\dot{x}_f^2\right)^{\frac{2}{\alpha+1}}(x_f - \xi)^{\frac{2}{\alpha+1}} + \cdots. \end{aligned} \tag{60}$$

Now we consider the momentum of the fluid in the tip region, $P(t)$. We have

$$\begin{aligned} P(t) &= \int_{\xi}^{x_f} h(x,t)u(x,t)dx \\ &= \int_{\xi}^{x_f} h(x,t)\left\{\dot{x}_f + u_1(t)\left(x_f - x\right) + \cdots\right\}dx \\ &= \dot{x}_f \int_{\xi}^{x_f} h(x,t)dx + u_1(t)\int_{\xi}^{x_f} h(x,t)(x_f - x)dx + \cdots . \end{aligned}$$

Upon differentiation with respect to t this becomes

$$\begin{aligned} \frac{dP}{dt} &= \ddot{x}_f \int_{\xi}^{x_f} h(x,t)dx + \dot{x}_f \frac{d}{dt}\left(\int_{\xi}^{x_f} h(x,t)\left(x_f - x\right)dx\right) + \cdots \\ &= \ddot{x}_f \int_{\xi}^{x_f} h(x,t)dx + \dot{x}_f\left(\dot{x}_f - \dot{\xi}\right)h(\xi,t) + \cdots . \end{aligned} \tag{61}$$

By (38) and the expansion for $u(x,t)$ at $x = \xi$ we also have

$$\frac{dP}{dt} = \dot{x}_f\left(\dot{x}_f - \dot{\xi}\right)h(\xi,t) + \cdots + F. \tag{62}$$

Now (61) and (62) give

$$\ddot{x}_f \int_{\xi}^{x_f} h(x,t)dx = F, \tag{63}$$

which is the same as in Whitham's Chézy case but with a different F. This is due to the first non-zero power of the u expansion being 1, meaning, like Whitham, we have taken the approximation $u = \dot{x}_f$. In turn this validates (46) for the the general α case and Whitham's argument follows identically except the F term is dependent on α.

Using (60) and the Ritter solution for $h(\xi,t)$, F may be written (from (40)) in terms of x_f and its derivatives as

$$F = \frac{1}{2}\left(1 - \frac{\dot{x}_f}{2}\right)^4 - \frac{1}{2}\left\{\left(\alpha+1\right)\dot{x}_f^2\left(x_f - \xi\right)\right\}^{\frac{2}{\alpha+1}} . \tag{64}$$

Using result (50) (which follows from the same argument as used earlier), substitution for F into (64) gives

$$\ddot{x}_f\left(1 - \frac{\dot{x}_f}{2}\right)^3 t = \frac{1}{2}\left(1 - \frac{\dot{x}_f}{2}\right)^4 - \frac{1}{2}\left\{\left(\alpha+1\right)\dot{x}_f^2\left(x_f - \xi\right)\right\}^{\frac{2}{\alpha+1}} .$$

Finally, substituting in for ξ from the Ritter solution (48), we obtain the non-linear ordinary differential equation

$$2\ddot{x}_f\left(1 - \frac{\dot{x}_f}{2}\right)^3 t = \left(1 - \frac{\dot{x}_f}{2}\right)^4 - \left\{\left(\alpha+1\right)\dot{x}_f^2\left(x_f - \left(\frac{3\dot{x}_f}{2} - 1\right)t\right)\right\}^{\frac{2}{\alpha+1}} . \tag{65}$$

When $\alpha = 1$, (65) is Whitham's Chézy equation (51). Comparing (51) and (65), the only difference is in the final term (resulting from the difference in horizontal resistance acting on the tip region) where an increasing α has a consequence of reducing both the power of $\dot{x}_f^2$ and the tip width $(x_f - \xi)$ by equal proportions. For a small tip region, the reduction of power will, overall, increase the magnitude of the friction term, and thus model larger friction at small times - which is as we would hope!

To solve (51), Whitham defines a variable d as $d(t) = 2t - x_f(t)$ (the difference in head position of the Ritter solution and x_f) and then makes a further change of variables $p = \dot{d}$ and $t = f'(p)$. This gives $d = pf'(p) - f(p)$ (easily checked with the chain rule) and $\ddot{d} = 1/f''(p)$. Now (51) becomes

$$4p^3 f' + p^4 f'' = 16(2-p)^2(pf' + 2f)f''. \tag{66}$$

This can be solved numerically with the help of solving the first few terms of the power series of f - this is useful to do since the initial conditions are $f(0) = f'(0) = 0$ and they will yield a trivial result. If we undergo the same change of variables in (65) we find

$$4p^3 f' + p^4 f'' = 16\left\{\left(\frac{\alpha+1}{2}\right)(2-p)^2(pf' + 2f)\right\}^{\frac{2}{\alpha+1}} f'', \tag{67}$$

with $f(0) = f'(0) = 0$. We seek a power series solution for $f(p)$ about $p = 0$. That is, suppose

$$f = f_0 p^\gamma + \cdots,$$

for constants f_0 and γ. Substitution into (67), at first order, gives

$$f_0\left(4\gamma + \gamma\left(\gamma - 1\right)\right)p^{\gamma+2} = 16\left\{2\left(\alpha+1\right)\left(\gamma+1\right)f_0 p^\gamma\right\}^{\frac{2}{\alpha+1}} f_0\gamma\left(\gamma-1\right)p^{\gamma-2}. \tag{68}$$

Equating the powers of p finds γ as

$$\gamma = 2\left(\alpha+1\right). \tag{69}$$

Substituting back into (68) we can solve for f_0 to find

$$f_0 = \frac{1}{4\left(\alpha+1\right)\left(\alpha+2\right)}\left(\frac{5+2\alpha}{16\left(2\alpha+1\right)}\right)^{\frac{\alpha+1}{2}}. \tag{70}$$

Hence, (69) and (70) give an approximation for $f(p)$ and $f'(p)$ as

$$f(p) = \frac{1}{4\left(\alpha+1\right)\left(\alpha+2\right)}\left(\frac{5+2\alpha}{16\left(2\alpha+1\right)}\right)^{\frac{\alpha+1}{2}} p^{2(\alpha+1)} + \cdots,$$

and

$$f'(p) = \frac{1}{2\left(\alpha+2\right)}\left(\frac{5+2\alpha}{16\left(2\alpha+1\right)}\right)^{\frac{\alpha+1}{2}} p^{2\alpha+1} + \cdots. \tag{71}$$

Now we can solve (67) numerically using the non-zero boundary conditions and avoid the trivial solution. Instead of using $f(0) = f'(0) = 0$ we can use the approximations for f and f' at some small p value, p_0 say, and take $f(p_0) \neq 0$, $f'(p_0) \neq 0$ as the boundary conditions. To check the accuracy of the approximated boundary conditions, we can use them to calculate the values for $f(0)$ and $f'(0)$ and confirm they are appropriately close to zero. It was found (using the MATLAB code in appendix B.2) that $p_0 = 0.05$ is sufficiently small. For example, solving (67) under Manning friction with $p_0 = 0.05$ gives $f(0) = 1.0345 \times 10^{-11}$ and $f'(0) = 9.4442 \times 10^{-9}$.

Plots for various α are displayed in figure 10 for comparison. It is clear that a larger α slows the front more rapidly.

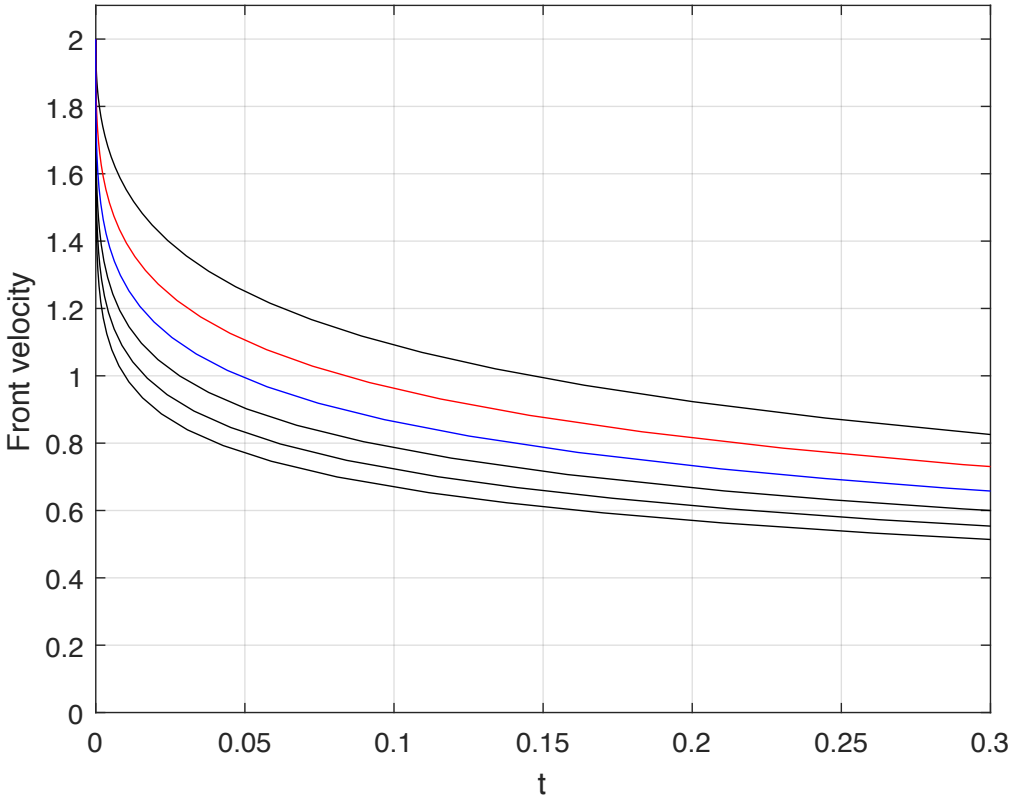

Figure 10: Solutions to (65) for values of α from 2/3 to 7/3 in increments of 1/3 (from top to bottom). In particular, the exact solution Whitham derived for Chézy friction is in red. The modified version for Manning friction is in blue.

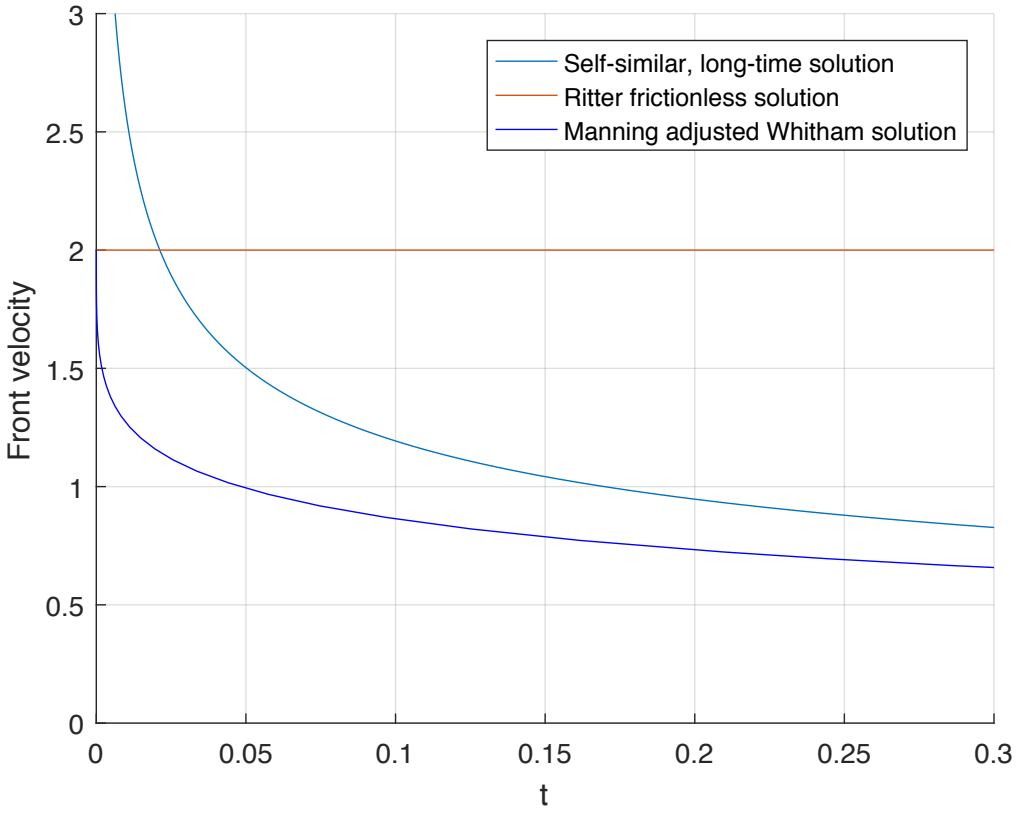

Figure 11: Comparison of solutions for front velocity.

5.3 Asymptotic behaviour of (65)'s solutions

Whitham found (as will be demonstrated below) that under Chézy friction, for small times

$$\dot{x}_f \sim 2 - 3.452t^{1/3}, \tag{72}$$

and for large times

$$\dot{x}_f \sim \left(\frac{1}{2t}\right)^{1/2}. \tag{73}$$

To find the small time behaviour for a general α, we use the first term of $f'(p)$ given in (71) to write

$$\begin{aligned} t = f'(p) &\sim \frac{1}{2\left(\alpha+2\right)}\left(\frac{5+2\alpha}{16\left(2\alpha+1\right)}\right)^{\frac{\alpha+1}{2}} p^{2\alpha+1} \\ &= \frac{1}{2\left(\alpha+2\right)}\left(\frac{5+2\alpha}{16\left(2\alpha+1\right)}\right)^{\frac{\alpha+1}{2}} \left(2-\dot{x}_f\right)^{2\alpha+1}. \end{aligned}$$

Rearranging, we find the short time asymptotic behaviour

$$\dot{x}_f \sim 2 - \left\{ 2\left(\alpha+2\right)\left(\frac{16\left(2\alpha+1\right)}{5+2\alpha}\right)^{\frac{\alpha+1}{2}} t \right\}^{\frac{1}{2\alpha+1}}. \tag{74}$$

Further, we can find the long time behaviour for general α predicted from this model by assuming the behaviour

$$f'(p) \sim C\left(2-p\right)^{-k}, \tag{75}$$

as $p \to 2$ for some $k > 0$ and constant C. For f and f'' this gives

$$f = \frac{C}{k-1}\left(2-p\right)^{1-k}, \tag{76}$$

$$f'' = Ck\left(2-p\right)^{-k-1}. \tag{77}$$

Substituting (75), (76) and (77) into (67) we have

$$4Cp^3\left(2-p\right)^{-k} + Ckp^4\left(2-p\right)^{-k-1} =$$
$$\frac{16Ck}{\left(2-p\right)^{k+1}}\left\{\left(\frac{\alpha+1}{2}\right)\left(2-p\right)^2\left(Cp\left(2-p\right)^{-k} + \frac{2C}{k-1}\left(2-p\right)^{1-k}\right)\right\}^{\frac{2}{\alpha+1}}.$$

Keeping the smallest (most dominant) powers of $(2-p)$ we must have

$$Ckp^4\left(2-p\right)^{-k-1} = 16Ck\left\{Cp\left(\frac{\alpha+1}{2}\right)\right\}^{\frac{2}{\alpha+1}}\left(2-p\right)^{\frac{2(2-k)}{\alpha+1}}\left(2-p\right)^{-k-1}, \tag{78}$$

and hence equating powers

$$-k-1 = \frac{2(2-k)}{\alpha+1} - k - 1,$$

giving

$$k = 2. \tag{79}$$

Equating the coefficients of the powers in (78) as $p \to 2$ we find

$$32C = 32C\left\{2C\left(\frac{\alpha+1}{2}\right)\right\}^{\frac{2}{\alpha+1}},$$

which rearranging for C gives

$$C = \frac{1}{\alpha+1}. \tag{80}$$

Substituting (79) and (80) back into (75) we have, for large time

$$t = f'(p) \sim \frac{1}{\alpha+1}\left(2-p\right)^{-2} = \frac{1}{\alpha+1}\left(\dot{x}_f\right)^{-2},$$

and so

$$\dot{x}_f \sim \left(\frac{1}{(\alpha+1)\,t}\right)^{1/2}. \tag{81}$$

Hence, although invalid for large time, all solutions from this method take the same power law as $t \to \infty$. Taking the natural logarithm of both sides gives

$$\ln(\dot{x}_f) = -\frac{1}{2}\ln(\alpha+1) - \frac{1}{2}\ln(t).$$

As α increases, $\ln(\alpha+1)$ increases. It follows then that solutions to (65) plotted on a $\ln(t)$ vs. $\ln(\dot{x}_f)$ graph will have the same gradient as $t \to \infty$ but the plots with larger α will lie below plots with smaller α. Also, (34) may be plotted on these axis (dependent on some $s_0(\alpha)$), with the expectation of a gradient of $-1/3$; shallower than that of the gradient of $-1/2$. These results are visible in figure (12) and confirm that Whitham's method of solving for the front velocity does indeed breakdown for large times.

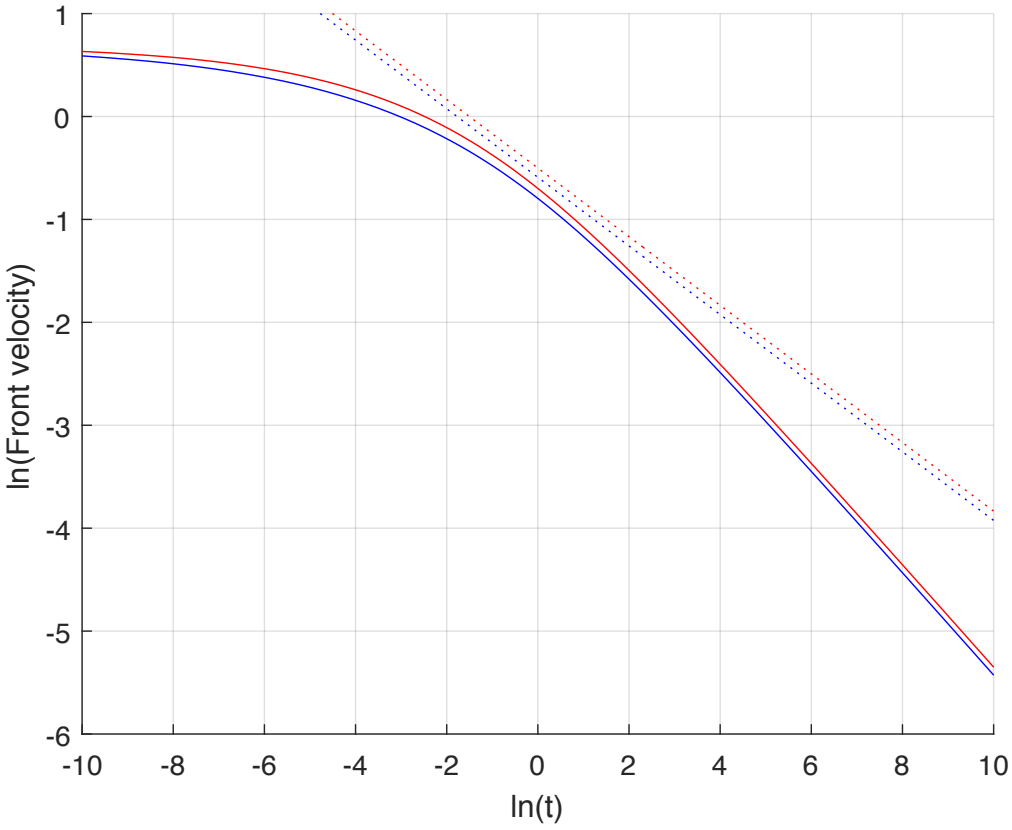

Figure 12: Comparison of front velocities on $\ln(t)$ vs. $\ln(\dot{x}_f)$ axes. Whitham's Chézy solution is in red and the Manning adjusted Whitham solution is in Blue. The self similarity solutions (34) are in dotted red and dotted blue for Chézy and Manning friction respectively.

5.4 Comparison of Manning and Chézy friction

From (74) and (81), letting $\alpha = 4/3$, we find for Manning friction that Whitham's method predicts for small times

$$\dot{x}_f \sim 2 - 3.206t^{3/11}, \tag{82}$$

and for large times

$$\dot{x}_f \sim \left(\frac{3}{7t}\right)^{1/2}. \tag{83}$$

Comparing (82) with the small time result derived by Whitham for Chézy friction (72), we see that for Manning friction the power of t is smaller and since both powers are less than one, for small t the Manning model predicts stronger decay of $\dot{x}_f$ and hence stronger friction.

It is disconcerting that the coefficient of the power of t is smaller for the Manning case (3.206...) than the Whitham case (3.452...), however, for small times the power takes dominance. The small time approximations for $\dot{x}_f$ can only be considered realistic for small p values since they were derived from the first term of the expansion for $f'(p)$ about $p = 0$ (t about $\dot{x}_f = 2$). Hence, by the time $\dot{x}_f$ has fallen to 1 we can expect the small time expressions to be invalid. Over such a small time scale, the power of t still has dominance over the coefficient. In fact, for Chézy and Manning friction the first term solutions are first equal (for $t > 0$) at $t = 0.2946...$, by which time the leading order predictions are vastly incorrect - even predicting negative $\dot{x}_f$ values!

5.5 Asymptotic behaviour at the back of the tip region

It was noticed after finding the asymptotic solutions above that as $t \to 0$ all the terms of the $h(x,t)$ expansion have the *same* asymptotic behaviour at the back of the tip region, $x = \xi$. Let the function $k(\alpha)$ simplify (74) as follows

$$\dot{x}_f \sim 2 - k(\alpha)t^{\frac{1}{2\alpha+1}}. \tag{84}$$

Now considering the Ritter solution (48) for $\xi(t)$ we may use (84) to write

$$\xi(t) = \left(\frac{3\dot{x}_f}{2} - 1\right)t \sim \left(3 - 1 - \frac{3k(\alpha)}{2}t^{\frac{1}{2\alpha+1}}\right)t = 2t - \frac{3k(\alpha)}{2}t^{\frac{2\alpha+2}{2\alpha+1}}. \tag{85}$$

We can also calculate the x_f and $\ddot{x}_f$ behaviours from (84) as

$$x_f \sim 2t - \left(\frac{2\alpha+1}{2\alpha+2}\right)k(\alpha)t^{\frac{2\alpha+2}{2\alpha+1}}, \tag{86}$$

$$\ddot{x}_f \sim \left(\frac{1}{2\alpha+1}\right)k(\alpha)t^{-\frac{2\alpha}{2\alpha+1}}. \tag{87}$$

From (85) and (86) we find for the tip width

$$x_f - \xi \sim \left\{ \frac{3k(\alpha)}{2} - \left(\frac{2\alpha+1}{2\alpha+2} \right) k(\alpha) \right\} t^{\frac{2\alpha+2}{2\alpha+1}} = \left(\frac{\alpha+2}{2\alpha+2} \right) k(\alpha) t^{\frac{2\alpha+2}{2\alpha+1}}. \quad (88)$$

We are now in a position to calculate the terms of $h(\xi, t)$. For the first term (from (59)) we find

$$\begin{aligned} \left((\alpha+1)\dot{x}_f^2 \left(x - \xi \right) \right)^{\frac{1}{\alpha+1}} &\sim \left(4(\alpha+1) \left(\frac{\alpha+2}{2\alpha+2} \right) k(\alpha) \right)^{\frac{1}{\alpha+1}} t^{\frac{2}{2\alpha+1}} \\ &= \left(2\left(\alpha+2\right) k(\alpha) \right)^{\frac{1}{\alpha+1}} t^{\frac{2}{2\alpha+1}}. \end{aligned} \quad (89)$$

From (59) we have for the second term (again, using (87) and (88))

$$\begin{aligned} \left(\frac{\alpha+1}{2\alpha+1} \right) \ddot{x}_f \left(x_f - \xi \right) &\sim \left(\frac{(\alpha+1)(\alpha+2)}{(2\alpha+1)^2(2\alpha+2)} \right) k(\alpha)^2 t^{-\frac{2\alpha}{2\alpha+1} + \frac{2\alpha+2}{2\alpha+1}} \\ &= \left(\frac{\alpha+2}{2(2\alpha+1)^2} \right) k(\alpha)^2 t^{\frac{2}{2\alpha+1}}. \end{aligned} \quad (90)$$

Thus by (89) and (90), the first two terms of h have the same asymptotic behaviour (to a constant of multiplication) as $t \to 0$.

If we consider the Ritter solution (36) for $h(x, t)$, using (85) we find

$$H(t) = h(\xi, t) = \frac{1}{9} \left(\frac{\xi}{t} - 2 \right)^2 \sim \frac{1}{9} \left(\frac{2t - \frac{3}{2} k(\alpha) t^{\frac{2\alpha+2}{2\alpha+1}}}{t} - 2 \right)^2 = \frac{k(\alpha)^2}{4} t^{\frac{2}{2\alpha+1}}. \quad (91)$$

Hence, the terms of the expansion for the height behave in the same manner as the Ritter solution as $t \to 0$ at $x = \xi$. Only using the first term leads to a discontinuity in height at $x = \xi$ between the expansion and the Ritter solution.

A more rigorous approximation for $h(x, t)$ in the tip region is found by Hogg and Pritchard (2004) [7] for Chézy friction. By writing the frictional shallow water equations (7) and (8) in an 'inner' variable $X = (x_f - x)/\epsilon$, with expansions of h and u about ϵ, the equations at $O(1)$ and $O(\epsilon)$ are rewritten using a similarity variable $\eta = X/(\eta_1 t^{(4/3)})$, where η_1 is a constant. These can then be integrated numerically, matching to the Ritter solution as $X \to -\infty$. The scaling for the leading order term of the h expansion was found by Hogg and Pritchard as $t^{2/3}$ - exactly that of the above results (89), (90) and (91) with $\alpha = 1$ (Chézy friction).

6 Rescaling

In this section we reintroduce dimensions into the obtained dimensionless results. All results were found in the frictional length and time scales so we convert back using (3) with (14) and (15).

Some previous results in dimensional variables are;

- Solutions for the front position and velocity (33) and (34) obtained using the similarity variable $s = xt^{2/3}$:

$$x_f = s_0 \left(C H_1^{\frac{\alpha+1}{2}} t \right)^{2/3}, \tag{92}$$

$$v_f = \frac{2s_0}{3} \left(\frac{C^2 H_1^{1+\alpha}}{t} \right)^{1/3}. \tag{93}$$

- Solutions for the small and large time asymptotics for the front velocity (84) and (81) using Whitham's method for a general α:

  As $t \to 0$

$$\dot{x}_f \sim (gH_1)^{1/2} \left\{ 2 - k(\alpha) \left(\frac{g^{3/2}}{C^2 H_1^{\alpha-\frac{1}{2}}} t \right)^{\frac{1}{2\alpha+1}} \right\}. \tag{94}$$

  As $t \to \infty$

$$\dot{x}_f \sim \left(\frac{C^2 H_1^{\alpha+1}}{(\alpha+1)(gH_1)^{1/2} t} \right)^{1/2}. \tag{95}$$

Additionally, all graphs presented in this study may have their axes dimensionalised. In particular, graphs which are of the form

$$s \text{ vs. } F(s) \quad \text{will become} \quad \frac{1}{C^{2/3} H_1^{(\alpha+1)/3}} x t^{-2/3} \quad \text{vs. } h(x,t)/H_1, \text{ and}$$

$$\bar{t} \text{ vs. } \bar{\dot{x}}_f \quad \text{will become} \quad \frac{g^{3/2}}{C^2 H_1^{\alpha-1/2}} t \quad \text{vs. } (gH_1)^{-1/2} \dot{x}_f.$$

7 Concluding Remarks

Various results related to the dam-break problem were found in this study. These include:

- New solutions for the dam-break problem as $t \to \infty$ (using ideas proposed by Daley and Porporato (2004) [6] to use similarity solutions for non-linear diffusion problems).
- Solving front speeds in the dry dam-break problem as $t \to \infty$ for general α.
- A generalisation of Whitham's solution for the front speed to accommodate general α.
- Showing that the generalisation of Whitham's solution found in this study (and thus also Whitham's original solution) for the front velocity is wrong as $t \to \infty$.

A possible continuation of this study would be to seek self-similar solutions using an inner variable located at the front of the flow (see Hogg and Pritchard (2004) [7]) to give a better approximation for the height profile of the tip.

8 Appendix

A Appendix A

A.1 Frictionless Shallow Water Equations

Assuming no Coriolis, viscous, or (most importantly) *friction* forces, the one dimensional shallow water equations for the depth-averaged velocity, $u(x,t)$, and height, $h(x,t)$, are

$$\begin{aligned} h_t + (uh)_x &= 0 \qquad \text{(mass conservation)}, \\ u_t + uu_x &= -gh_x \quad \text{(momentum conservation)}. \end{aligned}$$

The one dimensional shallow water equations are derived from the two dimensional Euler equations and hold when $H/L \ll 1$, where H is a typical height for the flow and L is a typical wavelength scale. Upon the assumption above that $H/L \ll 1$, it may be shown by balancing terms in Euler's vertical momentum equation that the vertical pressure varies hydrostatically. Euler's momentum equation can then be integrated over depth h to deduce the shallow water momentum equation above.

Integrating Euler's mass conservation equation ($\nabla \cdot u = 0$) over depth and applying the boundary and kinematic conditions then gives the shallow water mass conservation equation. A full derivation can be found in many textbooks, among such is Acheson's 'Elementary Fluid Dynamics' [10].

A.2 Secant method

For a function $f(x)$ say, and two initial values x_0 and x_1, the *secant method* is a root finding method defined by the recurrence relation

$$x_n = x_{n-1} - f(x_{n-1})\frac{x_{n-1} - x_{n-2}}{f(x_{n-1}) - f(x_{n-2})}.$$

A.3 Ritter solution for the frictionless shallow water equations

Ritter (1892) [1] solved the frictionless shallow water equations (see appendix A.1) using the method of characteristics. Here we do the same. To begin we let $c(x,t) = (gh(x,t))^{1/2}$ and the equations may be written

$$\begin{aligned} \left[\frac{\partial}{\partial t} + (u+c)\frac{\partial}{\partial x}\right](u+2c) = 0, \\ \left[\frac{\partial}{\partial t} + (u-c)\frac{\partial}{\partial x}\right](u-2c) = 0. \end{aligned}$$

Hence, the method of characteristics deduces that $u \pm 2c$ is constant along the characteristic curves $\dot{x} = u \pm c$.

Now consider the dry dam-break set-up with height H_1 behind the dam. For the undisturbed region in $x < 0$, the above gives $u \pm 2c = 2c_1$ along $\dot{x} = u \pm c_1$, where $c_1 = (gH_1)^{1/2}$. Hence, $u = 0$ and $c = c_1$ along $\dot{x} = \pm c_1$. So in the undisturbed region, the characteristic curves are straight lines with gradient $\pm c_1 t$ and the region is bounded by the curve emanating from $x = 0$. i.e $x = -c_1 t$.

Any point to the right of $x = -c_1 t$ will lie on a positive characteristic emanating from the undisturbed region - hence $u + 2c = 2c_1$. From the negative characteristic we have $u - 2c = k$ for some unknown constant k. Combining these two results it is clear that u and c are constant along the negative characteristic and $\dot{x} = u - c$ is a line of constant slope. Different characteristics have different k values and therefore the negative characteristics cross. The only reasonable place for this to happen is at the

origin (since there is an initial discontinuity there). Thus the negative characteristics take the form $u - c = x/t$. Since the '$u + 2c = 2c_1$' positive characteristic equality holds everywhere, we can solve

$$u - c = \frac{x}{t},$$
$$u + 2c = 2c_1,$$

to give the solution of the 'disturbed' region

$$u(x,t) = \frac{2}{3}\left(c_1 - \frac{x}{t}\right),$$
$$c(x,t) = \frac{1}{3}\left(2c_1 - \frac{x}{t}\right).$$

Reintroducing g, h and h_0 gives the *Ritter solution*. The front position can be found by solving for $h = 0$, which gives $x = 2\left(gH_1\right)^{1/2}$t. Obviously there is no fluid ahead of this point.

B MATLAB codes

B.1 MATLAB code to solve (12)

Below is the code used to solve and plot the solution for the wet and dry dam-break problem under general α.

Script file

```
%script solving the similarity solution for the dam break problem
%input variables: alpha        :friction strength
%                 height_left  :initial height behind the dam
%                 height_right :initial height infront the dam
%                 [sl,sr]      :domain the full eqn is being solved on
%                                (the points where B.Cs are applied)
%                 tol          :tolerence of secant method
%                 d            :how much linearised solution is plotted
%                                (plots are over [d*sl,d*sr])
%                 col          :colour and style of plots
%                 eps          :in dry case this is the distance from
%                               the front at which height and gradient
%                               are established
alpha=1; height_left=1; height_right=0; sl=-10; sr=-sl; tol=10^(-9);
ODE=@(x,y) F_ode(x,y,alpha); d=1; col='b'; eps=10^(-12);
if (height_right>0)  %wet dam break
    A0=14.9;         %guesses for unknown LHS constant, A
    A1=15;           %(need to be close enough for script to work!)
    hl = @(A) height_lin(A,height_left,sl,alpha);
    gl = @(A) grad_lin(A,height_left,sl,alpha);
    f  = @(A) hdifference(ODE,sl,sr,feval(hl,A),feval(gl,A),...
                          height_right,alpha);
    A  = secant(A0,A1,f,tol);
%plot on [sl,sr]
    plot_sol(A,hl,gl,sl,sr,ODE,col); hold on
%plot at the far ends (linearised solution)
```

```
    plot_lin_sols(A,sl,sr,height_left,height_right,ODE,alpha,d,col)
else                    %dry dam break
     s0_0=0.8;          %guesses for the front s0
     s0_1=0.9;
     sr   = @(s0) s0-eps;
     hloc= @(s0) h_loc(s0,eps,alpha); gloc=@(s0) g_loc(s0,eps,alpha);
     f    = @(s0) hdifference(ODE,feval(sr,s0),sl,feval(hloc,s0),...
                              feval(gloc,s0),height_left,alpha);
     s0=secant(s0_0,s0_1,f,tol);
%plots on [sl,s0-eps) and [s0,-sl*d]
     plot_zero_sol(sl,s0,eps,ODE,hloc,gloc,col); hold on
     plot_zero(s0,sl,d,col)
     if (d>1)           %plot on [d*sl,sl]
         plot_lin_zero_sol(sl,s0,eps,height_left,ODE,alpha,hloc,...
                           gloc,d,col)
     end
end
axis([d*sl,-d*sl,0,1.2*height_left]); grid on
```

Function files:

```
%returns constant of integration based on height gradient
function f = Bvalue(h,gr,sr,alpha)
f=3*(h^(alpha+2)/(abs(gr)))^(1/2)-sr^2;
end
```

```
%second order system to be solved
function f = F_ode(x,y,alpha)
f = zeros(2,1);
f(1) = y(2);
f(2) = -(4/3)*x*y(2)*(abs(y(2)))^(1/2)/(abs((y(1)))^((alpha/2)+1))...
       - (alpha+2)*((y(2))^2)/y(1);
end
```

```
%local gradient approximation near s0
function f = g_loc(s0,eps,alpha)
f = -(1/(1+alpha))*(((4*s0^2)/9)*(alpha+1))^(1/(1+alpha))...
    *eps^(-alpha/(1+alpha));
end
```

```
%apprx gradient at large |s|
function f = grad_lin(A,h,s,alpha)
f = -(9*h^(alpha+2)/((s^2+A)^2));
end
```

```
%local height approximation near s0
function f = h_loc(s0,eps,alpha)
f =((4*s0^2/9)*(alpha+1)*eps)^(1/(1+alpha));
end
```

```
%difference at sr between
% (1)-the immediate height value from ode45, and
% (2)-the required height value calculated from the gradient at sr
function f = hdifference(ODE,sl,sr,hl,gl,height_right,alpha)
[x,y] = ode45(ODE,[sl,sr],[hl,gl]);
    p = length(x); hr = y(p,1); gr = y(p,2);
    B=Bvalue(height_right,gr,sr,alpha);
    f=height_lin(B,height_right,sr,alpha)-hr;
end
%NOTE: in the dry dam, implied right/left orientation is flipped
%      and ode45 is solving 'backwards'
```

```
%apprx height at large |s|
function f = height_lin(A,h,s,alpha)
if A>0
    f = h-(9*h^(alpha+2))/(2*(A^(3/2))).*((s./(A^(1/2))./...
        ((s.^2)/A+1)+atan(s./(A^(1/2)))-(abs(s)./s).*(pi/2));
elseif A<0
    f = h+(9*h^(alpha+2))/(4*(abs(A)^(3/2))).*((2.*s/abs(A)^(1/2)).*...
        (s.^2/abs(A)-1)-log(abs((s+(abs(A))^(1/2)).*...
        (s-((abs(A))^(1/2))))));
elseif A==0
    f = h-3*h^(alpha+2)./s.^3;
end
```

```
%secant method to find roots of function f
function x = secant(xnew,xold,f,tol)
while (abs(feval(f,xnew)) > tol)
    fold=feval(f,xold);
    fnew=feval(f,xnew);
    Anext=xnew-fnew*(xnew-xold)/(fnew-fold);
    xold=xnew; xnew=Anext;
end
x = xnew;
```

```
function plot_lin_sols(A,sl,sr,height_left,height_right,ODE,alpha,d,
   colour)
   %plot on [d*sl, sl]
slow=d*sl; sup=sl;
s=slow:0.05:sup;
plot(s,height_lin(A,height_left,s,alpha),colour)
   % plot on [sr,d*sr]...
slow=sr; sup=d*sr;
[x,y] = ode45(ODE,[sl,sr],[height_lin(A,height_left,sl,alpha),...
                           grad_lin(A,height_left,sl,alpha)]);
p = length(x); gr = y(p,2);
B=Bvalue(height_right,gr,sr,alpha);
s=slow:0.05:sup;
plot(s,height_lin(B,height_right,s,alpha),colour)
end
```

```
function plot_lin_zero_sol(sl,s0,eps,height_left,ODE,alpha,hloc,...
                           gloc,d,colour)
h=feval(hloc,s0); g=feval(gloc,s0);
[x,y]=ode45(ODE,[s0-eps,sl],[h,g]);
A=Bvalue(height_left,y(length(x),2),sl,alpha);
slow=d*sl; sup=sl;
s=[slow,sup];
plot(s,height_lin(A,height_left,s,alpha),colour)
end
```

```
function plot_sol(A,hl,gl,sl,sr,ODE,colour)
h=feval(hl,A); g=feval(gl,A);
[x, y] = ode45(ODE,[sl,sr],[h,g]);
plot(x,y(:,1),colour)
end
```

```
function plot_zero_sol(sl,s0,eps,ODE,hloc,gloc,colour)
[x,y]=ode45(ODE,[s0-eps,sl],[feval(hloc,s0),feval(gloc,s0)]);
plot(x,y(:,1),colour)
end
```

```
function plot_zero(s0,sl,d,colour)
x=s0:0.05:-sl*d;
y=0.*x;
plot(x,y,colour)
end
```

B.2 MATLAB code to solve (65)

Below is the code used to solve and plot (65) for the predicted wavefront velocity under general α strength friction using Whitham's method.

Script file:

```
%solving gen alpha Whitham eqn for front
%Input variables: alpha: friction strength
%                 col  : colour and style of plots
%                 p    : point at which B.Cs are evaluated
alpha=4/3; col='b'; p = 0.05;
[x, y] = ode45(@(x,y) whitham_gen_alpha_ode(x,y,alpha), [p 2],...
    [f_apprx_gen_alpha(p,alpha) f_prime_apprx_gen_alpha(p,alpha)]);
plot(y(:,2),2-x,col)    %Plot for 't' vs. 'front velocity'
axis([0,0.3,0,2.1])
hold on;
%to plot the small section on [0,p]
[x, y] = ode45(@(x,y) whitham_gen_alpha_ode(x,y,alpha), [p 0],...
    [f_apprx_gen_alpha(p,alpha) f_prime_apprx_gen_alpha(p,alpha)]);
plot(y(:,2),2-x,col); xlabel('t'); ylabel('Front velocity')
grid on
```

Function files:

```
%first terms of power series for f(p) in gen alpha case
function f = f_apprx_gen_alpha(p,alpha)
f = (1/(4*(alpha+1)*(alpha+2)))*((5+2*alpha)/...
    (16*(2*alpha+1)))^((alpha+1)/2).*p.^(2*(alpha+1));
end
```

```
%first term for power series of f'(p) in gen alpha case
function f = f_prime_apprx_gen_alpha(p,alpha)
f = (1/(2*(alpha+2)))*((5+2*alpha)/...
    (16*(2*alpha+1)))^((alpha+1)/2).*p.^(2*alpha+1);
end
```

```
%second order system for the front under general alpha
%NOTE: this is in variables f(p) and p=d(2t-x_f)/dt
function f = whitham_gen_alpha_ode(p,y,alpha)
f = zeros(2,1);
f(1)=y(2);
f(2)=4*p.^3.*y(2)/(16*(((alpha+1)/2).*...
    (2-p).^2.*(p*y(2)+2*y(1))).^(2/(alpha+1))-p.^4);
end
```

References

[1] A Ritter. Die fortpflanzung der wasserwellen. *Vereine Deutscher Ingenieure Zeitschrift*, 36:947–954, 1892.

[2] R F Dressler. Hydraulic resistance effect upon the dam-break functions. *Journal of Research of the National Bureau of Standards*, 49:217–225, 1952.

[3] G B Whitham. The effects of hydraulic resistance in the dam-break problem. *Proceedings of the Royal Society of London A: Mathematical, Physical and Engineering Sciences*, 227(1170):399–407, 1955.

[4] C Ancey, R M Iverson, M Rentschler, and R P Denlinger. An exact solution for idea dam-break floods on steep slopes. *Water Resources Research*, 44, 2008.

[5] H Chanson. Application of the method of characteristics to the dam break wave problem. *Journal of Hydraulic Research*, 47:1:41–49, 2009.

[6] Edoardo Daly and Amilcare Porporato. Similarity solutions of nonlinear diffusion problems related to mathematical hydraulics and the fokker-planck equation. *Physical Review E*, 70:056303, Nov 2004.

[7] A J Hogg and D Pritchard. The effects of hydraulic resistance on dam-break and other shallow inertial flows. *Journal of Fluid Mechanics*, 501:179–212, 2004.

[8] Vincent Guinot. *Wave Propagation in Fluids : models and numerical techniques*. John Wiley and Sons, Inc, 2006.

[9] G. Gioia and F. A. Bombardelli. Scaling and similarity in rough channel flows. *Physical Review Letters*, 88:014501, Dec 2001.

[10] D J Acheson. *Elementary Fluid Dynamics*. Oxford University Press, Oxford, 1990.